**Geomechanics and Engineering**, *Vol. 14, No. 6 (2018) 519-532*
DOI: https://doi.org/10.12989/gae.2018.14.6.519


# Novel quasi-3D and 2D shear deformation theories for bending and free vibration analysis of FGM plates

Abderahman Younsi[1], Abdelouahed Tounsi[*1,2,3], Fatima Zohra Zaoui[4], Abdelmoumen Anis Bousahla[1,2,3] and S.R. Mahmoud[5]

[1]*Material and Hydrology Laboratory, University of Sidi Bel Abbes, Faculty of Technology, Civil Engineering Department, Algeria*
[2]*Laboratory of Structures and Advanced Materials in Civil Engineering and Public Works, Department of Civil Engineering, Faculty of Technology, University of Sidi Bel Abbes, Algeria*
[3]*Multi-scale Modeling and Simulation Laboratory, Department of Physics, Faculty of Exact Sciences, University of Sidi Bel Abbés, Algeria*
[4]*Laboratory for Numerical and Experimental Modeling of Mechanical Phenomena, Faculty of Sciences and Technology, Department of Mechanical Engineering, University Abdelhamid Ibn Badis of Mostaganem, 27000, Algeria*
[5]*Department of Mathematics, Faculty of Science, King Abdulaziz University, Saudi Arabia*

*(Received May 15, 2017, Revised September 26, 2017, Accepted October 11, 2017)*

**Abstract.** In this work, two dimensional (2D) and quasi three-dimensional (quasi-3D) HSDTs are proposed for bending and free vibration investigation of functionally graded (FG) plates using hyperbolic shape function. Unlike the existing HSDT, the proposed theories have a novel displacement field which include undetermined integral terms and contains fewer unknowns. The material properties of the plate is inhomogeneous and are considered to vary continuously in the thickness direction by three different distributions; power-law, exponential and Mori-Tanaka model, in terms of the volume fractions of the constituents. The governing equations which consider the effects of both transverse shear and thickness stretching are determined through the Hamilton's principle. The closed form solutions are deduced by employing Navier method and then fundamental frequencies are obtained by solving the results of eigenvalue problems. In-plane stress components have been determined by the constitutive equations of composite plates. The transverse stress components have been determined by integrating the 3D stress equilibrium equations in the thickness direction of the FG plate. The accuracy of the present formulation is demonstrated by comparisons with the different 2D, 3D and quasi-3D solutions available in the literature.

**Keywords:** bending; vibration; functionally graded plate; shear deformation theory; stretching effect

## 1. Introduction

Functionally graded materials (FGMs) are a kind of advanced composite materials whose properties change gradually and continuously from one surface to another. The mechanical characteristics of FGM change along the thickness direction in the material depending on a function. Because of this this feature, the FGMs have some benefits such as eliminating the material discontinuity and avoiding the delamination failure, diminishing the stress levels and deflections. Combination of these properties attracts application of FGMs in many engineering areas from biomedical to civil engineering (Ahmed 2014, Swaminathan and Naveenkumar 2014, Hadji *et al.* 2015, 2016, Abdelhak *et al.* 2016, Ahouel *et al.* 2016, Ghorbanpour Arani *et al.* 2016a, b, Aldousari 2017, Rahmani *et al.* 2017).

In recent years, FGM applications have received important increase. The increase in FGM applications requires accurate theories to examine their response (Bessaim *et al.* 2013, Tounsi *et al.* 2013, Zemri *et al.* 2015, Ait Atmane *et al.* 2015, Attia *et al.* 2015, Belkorissat *et al.* 2015, Larbi Chaht *et al.* 2015, Hamidi *et al.* 2015, Hebali *et al.* 2016, Barati and Shahverdi 2016, Barka *et al.* 2016, Beldjelili *et al.* 2016, Meksi *et al.* 2017, Menasria *et al.*, 2017). The bending and vibration behavior of FG plates have been investigated by many researchers in recent ten years. Kashtalyan (2004) presented a 3D elasticity solution for a simply supported FG plate under the transverse loading. Matsunaga (2009) developed a 2D higher-order theory for the prediction of displacement and stresses in FG plates under thermal and mechanical loadings. The model can take into account the influence of both transverse shear and normal stresses. Zhao *et al.* (2009) analyzed the free vibration of FG plates using the element-free kp-Ritz method. The first-order shear deformation plate theory (FSDT) is utilized to consider the transverse shear strain and rotary inertia, and mesh-free kernel particle functions are employed to approximate the 2D displacement fields. Vaghefi *et al.* (2010) proposed a version of meshless local Petrov-Galerkin procedure to determine 3D static solutions for thick FG plates. Orakdogen *et al.* (2010) examined the coupling influence of extension and static in FG plate under transverse loading for Kirchhoff-Love plate theory equations. Tamijani and Kapania (2012) presented an element free Galerkin method for the vibration of a FG plate with curvilinear stiffeners. The governing equations

∗Corresponding author, Professor
E-mail: tou_abdel@yahoo.com



ISSN: 2005-307X (Print), 2092-6219 (Online)

for the plate and stiffeners are obtained by employing the FSDT. Gunes *et al.* (2014) presented an experimental study about the low-velocity impact response of FG clamped circular plates. Zhang *et al.* (2014) proposed a 3D elasticity solution for bending of thick FG plates by using a hybrid semi-analytical approach-the state-space based differential quadrature method. Ait Amar Meziane *et al.* (2014) presented an efficient and simple refined theory for buckling and free vibration of exponentially graded sandwich plates under various boundary conditions. Ait Yahia *et al.* (2015) analyzed wave propagation in FG plates with porosities using various higher-order shear deformation plate theories. Sofiyev and Kuruoglu (2015) developed a theoretical formulation to solve dynamic problems of FG truncated conical shells under mixed boundary conditions. Zafarmand and Kadkhodayan (2015) studied the 3D bending and dynamic response of a thick sector plate made of two-directional FGMs. Kar and Panda (2015a) investigated the free vibration responses of temperature dependent FG curved panels under thermal environment. Kar and Panda (2015b) presented large deformation bending analysis of FG spherical shell using FEM. Kar and Panda (2015c) discussed nonlinear flexural vibration of shear deformable FG spherical shell panel. Kar *et al.* (2015) studied also the nonlinear flexural analysis of laminated composite flat panel under hygro-thermo-mechanical loading. Zhu and Liew (2011) presented free vibration analyses of FG plates with the local Kriging meshless method.

It is clear that non-negligible shear deformations occur at the thick and moderately thick plates and the classical plate theory (CPT) provides inaccurate results. So, transverse shear deformations have to be considered in the analysis. There is numerous plate models that introduce transverse shear strains for the advanced composites like FGMs. Benachour *et al.* (2011) developed a four variable refined plate theory for free vibration investigation of plates made of FGMs with an arbitrary gradient. Hosseini-Hashemi *et al.* (2011) proposed a novel exact closed-form method to solve free vibration analysis of FG rectangular thick plates based on the Reddy's third-order shear deformation plate theory while the plate has two opposite edges simply supported. Matsunaga (2008) investigated the natural frequencies and buckling stresses of FG plates by considering the effects of transverse shear and normal deformations and rotatory inertia. Jha *et al.* (2013) discussed the free vibration behavior of FG elastic, rectangular, and simply supported plates based on higher order shear/shear-normal deformations theories. Sheikholeslami and Saidi (2013) investigated the free vibration of simply supported FG rectangular plates resting on two-parameter elastic foundation using the higher-order shear and normal deformable plate theory. Hebali *et al.* (2014) developed a novel quasi-3D hyperbolic shear deformation theory for bending and free vibration analysis of FG plates. Belabed *et al.* (2014) proposed an efficient and simple higher order shear and normal deformation theory for FG plates. Alijani and Amabili (2014) studied the nonlinear forced vibrations of moderately thick FG rectangular plates by considering HSDTs that consider the thickness deformation effect. Akavci and Tanrikulu (2015) presented a new quasi-3D hyperbolic shear deformation theory for static and free vibration analysis of FG plates. Houari *et al.* (2016) presented a new simple three -unknown sinusoidal shear deformation theory for FG plates. Baseri *et al.* (2016) presented an analytical solution for buckling of embedded laminated plates based on higher order shear deformation plate theory. Kolahchi and Moniri Bidgoli (2016) used a sinusoidal beam model for dynamic instability of single-walled carbon nanotubes. Arani and Kolahchi (2016) analyzed buckling behavior of embedded concrete columns armed with carbon nanotubes. Kolahchi *et al.* (2016a) employed differential cubature and quadrature-Bolotin methods for dynamic stability of embedded piezoelectric nanoplates based on visco-nonlocal-piezoelasticity theories. Bilouei *et al.* (2016) investigated the buckling of concrete columns retrofitted with nano-fiber reinforced polymer. Madani *et al.* (2016) presented a differential cubature method for vibration analysis of embedded FG-CNT-reinforced piezoelectric cylindrical shells subjected to uniform and non-uniform temperature distributions. Kolahchi *et al.* (2016b) analyzed the dynamic stability of temperature-dependent functionally graded CNT-reinforced visco-plates resting on orthotropic elastomeric medium. Kolahchi *et al.* (2017) presented visco-nonlocal-refined Zigzag theories for dynamic buckling of laminated nanoplates using differential cubature-Bolotin methods. Zamanian *et al.* (2017) discussed the agglomeration effects on the buckling behavior of embedded concrete columns reinforced with SiO2 nano-particles. Bennoun *et al.* (2016) presented a novel five variable refined plate theory for vibration analysis of functionally graded sandwich plates. Ait Atmane *et al.* (2017) studied the effect of thickness stretching and porosity on mechanical response of a FG beams resting on elastic foundations. Benahmed *et al.* (2017) proposed a novel quasi-3D hyperbolic shear deformation theory for FG thick rectangular plates on elastic foundation. Benbakhti *et al.* (2016) developed also a new five unknown quasi-3D type HSDT for thermomechanical bending analysis of FGM sandwich plates. Chikh *et al.* (2017) discussed the thermal buckling response of cross-ply laminated plates using a simplified HSDT. Klouche *et al.* (2017) presented an original single variable shear deformation theory for buckling analysis of thick isotropic plates. Draiche *et al.* (2017) proposed a refined theory with stretching effect for the flexure analysis of laminated composite plates. Benchohra *et al.* (2017) presented a novel quasi-3D sinusoidal shear deformation theory for FG plates.

In this study, a novel quasi-3D hyperbolic shear deformation theory is proposed for bending and vibration investigation of FG plates. The developed theory provides good accuracy and considers a parabolic transverse shear deformation shape function and respects shear stress free boundary conditions of upper and lower surfaces of the plate without employing shear correction factors. Besides, the model considers the thickness stretching effect by employing the same hyperbolic function. By introducing integral terms in the in-plane displacements, the number of unknowns of the theory is reduced, thus saving computational time (Bourada *et al.* 2016). Governing equations are obtained from the Hamilton's principle. Navier solution is employed to determine the analytical solutions for simply supported FG plates. The in-plane stresses are computed from the linear constitutive relations

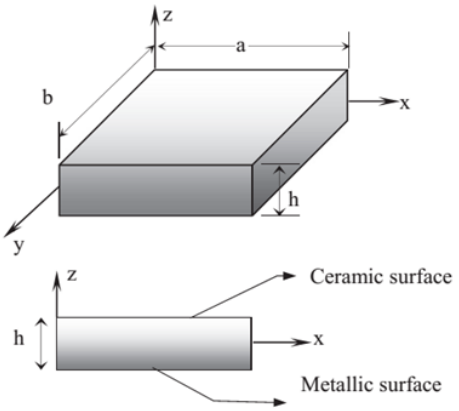


Fig. 1 Geometry and coordinates of the considered single-layer FGM plate

and the transverse shear and normal stresses are calculated by integrating the 3D stress equilibrium equations of elastic media by respecting the stress boundary conditions on the upper and lower surfaces of a plate. Numerical results are presented to demonstrate the accuracy and efficiency of the proposed theory.

## 2. Theoretical formulation

Consider a FG rectangular plate, having uniform thickness $h$, length $a$, width $b$ (Fig. 1).

In this work, the compositions and volume fractions of the constituents in FGM are assumed to change gradually across the thickness according to: (a) The power-law variation, (b) The exponential distribution, (c) The Mori-Tanaka homogenization model. Since the influences of Poisson's ratio $\nu$ on the response of FG plates are very small, it is supposed to be constant for all gradation models (Bouderba *et al.* 2013 and 2016, Bousahla *et al.* 2014 and 2016, Meradjah *et al.* 2015, Mouaici *et al.* 2016, Chikh *et al.* 2016, Bourada *et al.* 2015, Mahi *et al.* 2015, Boukhari *et al.* 2016, Zidi *et al.* 2014 and 2017).

a) The power-law (P-FGM) variation

The volume fraction of the P-FGM plate is considered to change continuously within the thickness of the plate in according to the power law variation (Bao and Wang 1995, Fekrar *et al.* 2014, Bellifa *et al.* 2016 and 2017. Benferhat *et al.* 2016, El-Hassar *et al.* 2016, Laoufi *et al.* 2016, Besseghier *et al.* 2017, Bouafia *et al.* 2017, El-Haina *et al.* 2017, Khetir *et al.* 2017, Mouffoki *et al.* 2017) as follows

$$P(z) = P_m + \left(P_c - P_m\right)\left(\frac{1}{2} + \frac{z}{h}\right)^k \tag{1}$$

b) The exponential (E-FGM) variation

The volume fraction of the E-FGM plate is considered to vary continuously within the thickness of the plate in according to the exponential variation (Delale and Erdogan, 1983) as follows

$$P(z) = Ae^{p\left(z+h/2\right)}, \quad A = P_m, \quad p = \frac{1}{h}\ln\left(\frac{P_c}{P_m}\right) \tag{2}$$

c) The Mori Tanaka homogenization model

For Mori-Tanaka scheme, the volume fraction of the FGM plate is given as (Mori and Tanaka 1973, Benveniste 1987, Belabed *et al.* 2014, Bounouara *et al.* 2016)

$$P(z) = P_m + \left(P_c - P_m\right)\frac{V_c}{1 + V_m\left(\frac{P_c}{P_m} - 1\right)\frac{1+\nu}{3-3\nu}}, \tag{3a}$$

with

$$V_c = \left(\frac{1}{2} + \frac{z}{h}\right)^k, \quad V_m + V_c = 1 \tag{3b}$$

where $P$ presents the effective material property like Young's modulus $E$, $P_m$ and $P_c$ denotes the property of the upper and the lower faces of the plate, respectively, $k$ is the power law index and $p$ is the volume fraction exponent.

### 2.1 Kinematics

On the basis of the thick plate theory and considering the thickness stretching influence, the supposed displacement field of the plate can be described as

$$u(x,y,z,t) = u_0(x,y,t) - z\frac{\partial w_0}{\partial x} + k_1 f(z)\int\theta(x,y,t)dx \tag{4a}$$

$$v(x,y,z) = v_0(x,y,t) - z\frac{\partial w_0}{\partial y} + k_2 f(z)\int\theta(x,y,t)dy \tag{4b}$$

$$w(x,y,z,t) = w_0(x,y,t) + g(z)\varphi(x,y,t) \tag{4c}$$

where $u_0$, $v_0$, $w_0$, $\theta$ and $\varphi_z$ are the five unknown displacement functions of middle surface of the plate. Note that the integrals do not have limits. The constants $k_1$ and $k_2$ depends on the geometry.

In this work, the shear strain shape functions are

$$f(z) = h\tanh^{-1}\left(\frac{z}{h}\right) - \left(\frac{4}{3}\right)^2\frac{z^3}{h^2}, \quad g(z) = \frac{df}{dz} \tag{5}$$

Based on the suppositions in Eq. (4), within the application of the linear, small-strain elasticity theory, the general strain-displacement relations are expressed as

$$\begin{Bmatrix}\varepsilon_x\\ \varepsilon_y\\ \gamma_{xy}\end{Bmatrix} = \begin{Bmatrix}\varepsilon_x^0\\ \varepsilon_y^0\\ \gamma_{xy}^0\end{Bmatrix} + z\begin{Bmatrix}k_x^b\\ k_y^b\\ k_{xy}^b\end{Bmatrix} + f(z)\begin{Bmatrix}k_x^s\\ k_y^s\\ k_{xy}^s\end{Bmatrix}, \quad \begin{Bmatrix}\gamma_{yz}\\ \gamma_{xz}\end{Bmatrix} = g(z)\begin{Bmatrix}\gamma_{yz}^0\\ \gamma_{xz}^0\end{Bmatrix}, \quad \varepsilon_z = g'(z)\varepsilon_z^0 \tag{6}$$

where

$$\begin{Bmatrix}\varepsilon_x^0\\ \varepsilon_y^0\\ \gamma_{xy}^0\end{Bmatrix} = \begin{Bmatrix}\frac{\partial u_0}{\partial x}\\ \frac{\partial v_0}{\partial x}\\ \frac{\partial u_0}{\partial y} + \frac{\partial v_0}{\partial x}\end{Bmatrix}, \quad \begin{Bmatrix}k_x^b\\ k_y^b\\ k_{xy}^b\end{Bmatrix} = \begin{Bmatrix}-\frac{\partial^2 w_0}{\partial x^2}\\ -\frac{\partial^2 w_0}{\partial y^2}\\ -2\frac{\partial^2 w_0}{\partial x\partial y}\end{Bmatrix}, \quad \begin{Bmatrix}k_x^s\\ k_y^s\\ k_{xy}^s\end{Bmatrix} = \begin{Bmatrix}k_1\theta\\ k_2\theta\\ k_1\frac{\partial}{\partial y}\int\theta\,dx + k_2\frac{\partial}{\partial x}\int\theta\,dy\end{Bmatrix} \tag{7a}$$

$$\begin{Bmatrix}\gamma_{yz}^0\\ \gamma_{xz}^0\end{Bmatrix} = \begin{Bmatrix}k_2\int\theta\,dy + \frac{\partial\varphi_z}{\partial y}\\ k_1\int\theta\,dx + \frac{\partial\varphi_z}{\partial x}\end{Bmatrix}, \quad \varepsilon_z^0 = \varphi_z \tag{7b}$$

and

$$g'(z)=\frac{dg(z)}{dz} \tag{7c}$$

It can be seen from equation (6) that the transverse shear strains ($\gamma_{xz}$, $\gamma_{yz}$,) are equal to zero at the top ($z=h/2$) and bottom ($z=-h/2$) surfaces of the plate. A shear correction coefficient is, hence, not required.

The integrals employed in the above equations shall be resolved by a Navier type method and can be expressed as follows

$$\frac{\partial}{\partial y}\int\theta\,dx=A'\frac{\partial^2\theta}{\partial x\partial y},\quad \frac{\partial}{\partial x}\int\theta\,dy=B'\frac{\partial^2\theta}{\partial x\partial y},\quad \int\theta\,dx=A'\frac{\partial\theta}{\partial x},\quad \int\theta\,dy=B'\frac{\partial\theta}{\partial y} \tag{8}$$

where the coefficients $A'$ and $B'$ are considered according to the type of solution employed, in this case via Navier method. Therefore, $A'$, $B'$, $k_1$ and $k_2$ are expressed as follows

$$A'=-\frac{1}{\alpha^2},\quad B'=-\frac{1}{\beta^2},\quad k_1=\alpha^2,\quad k_2=\beta^2 \tag{9}$$

where $\alpha$ and $\beta$ are defined in expression (20).

The linear constitutive relations of a FG plate according to the 3D elasticity can be written as

$$\begin{Bmatrix}\sigma_x\\ \sigma_y\\ \sigma_z\\ \tau_{xy}\\ \tau_{xz}\\ \tau_{yz}\end{Bmatrix}=\begin{bmatrix}C_{11}&C_{12}&C_{13}&0&0&0\\ C_{12}&C_{22}&C_{23}&0&0&0\\ C_{13}&C_{23}&C_{33}&0&0&0\\ 0&0&0&C_{66}&0&0\\ 0&0&0&0&C_{55}&0\\ 0&0&0&0&0&C_{44}\end{bmatrix}\begin{Bmatrix}\varepsilon_x\\ \varepsilon_y\\ \varepsilon_z\\ \gamma_{xy}\\ \gamma_{xz}\\ \gamma_{yz}\end{Bmatrix} \tag{10}$$

The elastic constants ($C_{ij}$) are depends on the normal strain $\varepsilon_z$.

• If the $\varepsilon_z\neq0$ then $C_{ij}$ are

$$C_{11}=C_{22}=C_{33}=\frac{(1-\nu)E(z)}{(1-2\nu)(1+\nu)}, \tag{11a}$$

$$C_{12}=C_{13}=C_{23}=\frac{\nu\,E(z)}{(1-2\nu)(1+\nu)}, \tag{11b}$$

$$C_{44}=C_{55}=C_{66}=\frac{E(z)}{2(1+\nu)}, \tag{11c}$$

• If the $\varepsilon_z=0$ then $C_{ij}$ are

$$C_{11}=C_{22}=\frac{E(z)}{(1-\nu^2)}, \tag{12a}$$

$$C_{12}=\frac{\nu\,E(z)}{(1-\nu^2)}, \tag{12b}$$

$$C_{44}=C_{55}=C_{66}=\frac{E(z)}{2(1+\nu)}, \tag{12c}$$

### 2.3 Equations of equilibrium and stress components

The Hamilton principle is considered herein to determine the equations of motion appropriate to the displacement field and the constitutive equations. The principle can be stated in analytical form as (Belabed *et al.* 2014, Taibi *et al.* 2015, Fahsi *et al.* 2017)

$$0=\int_0^t(\delta U+\delta V_p-\delta K)\,dt \tag{13}$$

where $\delta U$ is the variation of strain energy; $\delta V_p$ is the potential energy of applied distributed transverse load and $\delta K$ is the variation of kinetic energy of FG plate.

The equations of motion can be obtained from Eq. (13) by integrating the displacement gradients by parts and setting the coefficients $\delta u_0$, $\delta v_0$, $\delta w_0$, $\delta\theta$ and $\delta\varphi_z$ zero separately

$$\begin{aligned}
&\delta u_0:\ \frac{\partial N_x}{\partial x}+\frac{\partial N_{xy}}{\partial y}=I_0\ddot{u}_0-I_1\frac{\partial\ddot{w}_0}{\partial x}+J_1k_1A'\frac{\partial\ddot{\theta}}{\partial x}\\
&\delta v_0:\ \frac{\partial N_y}{\partial y}+\frac{\partial N_{xy}}{\partial x}=I_0\ddot{v}_0-I_1\frac{\partial\ddot{w}_0}{\partial y}+J_1k_2B'\frac{\partial\ddot{\theta}}{\partial y}\\
&\delta w_0:\ \frac{\partial^2M_x^b}{\partial x^2}+\frac{\partial^2M_y^b}{\partial y^2}+2\frac{\partial^2M_{xy}^b}{\partial x\partial y}+q=I_0\ddot{w}_0+J_0\ddot{\phi}+I_1(\frac{\partial\ddot{u}_0}{\partial x}+\frac{\partial\ddot{v}_0}{\partial y})-I_2\nabla\ddot{w}_0+J_2(k_1A'\frac{\partial^2\ddot{\theta}}{\partial x^2}+k_2B'\frac{\partial^2\ddot{\theta}}{\partial y^2})\\
&\delta\theta:\ -k_1M_x^s-k_2M_y^s-(k_1A'+k_2B')\frac{\partial^2M_{xy}^s}{\partial x\partial y}+k_1A'\frac{\partial S_{xz}^s}{\partial x}+k_2B'\frac{\partial S_{yz}^s}{\partial y}=-J_1(k_1A'\frac{\partial\ddot{u}_0}{\partial x}+k_2B'\frac{\partial\ddot{v}_0}{\partial y})\\
&\qquad+J_2(k_1A'\frac{\partial^2\ddot{w}_0}{\partial x^2}+k_2B'\frac{\partial^2\ddot{w}_0}{\partial y^2})-K_2((k_1A')^2\frac{\partial^2\ddot{\theta}}{\partial x^2}+(k_2B')^2\frac{\partial^2\ddot{\theta}}{\partial y^2})\\
&\delta\varphi_z:\ \frac{\partial S_{xz}^s}{\partial x}+\frac{\partial S_{yz}^s}{\partial y}-N_z=J_0\ddot{w}_0+K_0\ddot{\varphi}_z
\end{aligned} \tag{14}$$

The stress and moment resultants which appeared in Eq. (8) are given by

$$\begin{Bmatrix}N_x\\ N_y\\ N_{xy}\\ M_x^b\\ M_y^b\\ M_{xy}^b\\ M_x^s\\ M_y^s\\ M_{xy}^s\\ N_z\end{Bmatrix}=\begin{bmatrix}A_{11}&A_{12}&0&B_{11}&B_{12}&0&B_{11}^s&B_{12}^s&0&X_{13}\\ A_{12}&A_{22}&0&B_{12}&B_{22}&0&B_{12}^s&B_{22}^s&0&X_{23}\\ 0&0&A_{66}&0&0&B_{66}&0&0&B_{66}^s&0\\ B_{11}&B_{12}&0&D_{11}&D_{12}&0&D_{11}^s&D_{12}^s&0&Y_{13}\\ B_{12}&B_{22}&0&D_{12}&D_{22}&0&D_{12}^s&D_{22}^s&0&Y_{23}\\ 0&0&B_{66}&0&0&D_{11}&0&0&D_{66}^s&0\\ B_{11}^s&B_{12}^s&0&D_{11}^s&D_{12}^s&0&H_{11}^s&H_{12}^s&0&Y_{13}^s\\ B_{12}^s&B_{22}^s&0&D_{12}^s&D_{22}^s&0&H_{12}^s&H_{22}^s&0&Y_{23}^s\\ 0&0&B_{66}^s&0&0&D_{66}^s&0&0&H_{66}^s&0\\ X_{13}&X_{23}&0&Y_{13}&Y_{23}&0&Y_{13}^s&Y_{23}^s&0&Z_{33}\end{bmatrix}\begin{Bmatrix}\frac{\partial u_0}{\partial x}\\ \frac{\partial v_0}{\partial y}\\ \frac{\partial u_0}{\partial y}+\frac{\partial v_0}{\partial x}\\ -\frac{\partial^2w_0}{\partial x^2}\\ -\frac{\partial^2w_0}{\partial y^2}\\ -2\frac{\partial^2w_0}{\partial x\,\partial y}\\ k_1\theta\\ k_2\theta\\ (k_1A'+k_2B')\frac{\partial^2\theta}{\partial x\partial y}\\ \varphi_z\end{Bmatrix} \tag{15a}$$

$$\begin{Bmatrix}S_{yz}^s\\ S_{xz}^s\end{Bmatrix}=\begin{bmatrix}A_{44}^s&0\\ 0&A_{55}^s\end{bmatrix}\begin{Bmatrix}k_2B'\dfrac{\partial\theta}{\partial y}+\dfrac{\partial\varphi_z}{\partial y}\\ k_1A'\dfrac{\partial\theta}{\partial x}+\dfrac{\partial\varphi_z}{\partial x}\end{Bmatrix} \tag{15b}$$

where the stiffness components and inertias are given as

$$(A_{ij},A_{ij}^s,B_{ij},D_{ij},B_{ij}^s,D_{ij}^s,H_{ij}^s)=\int_{-h/2}^{h/2}Q_{ij}\left(1,g^2(z),z,z^2,f(z),z\,f(z),f^2(z)\right)dz \tag{16a}$$

$$(X_{ij},Y_{ij},Y_{ij}^s,Z_{ij})=\int_{-h/2}^{h/2}(1,z,f(z),g'(z))g'(z)Q_{ij}\,dz \tag{16b}$$

$$(I_0,I_1,I_2,J_1,J_2,J_0,K_0,K_2)=\int_{-h/2}^{h/2}(1,z,z^2,f,zf,g,g^2,f^2)\rho(z)\,dz \tag{16c}$$

and $\rho(z)$ is the mass density.

The in-plane normal and shear stresses ($\sigma_x$, $\sigma_y$ and $\tau_{xy}$) can be determined accurately by the constitutive relations (10) for FG plates. But if the transverse shear stresses ($\tau_{yz}$ and $\tau_{xy}$) computed from the constitutive relations (10), they may not respect the boundary conditions at the upper and lower surfaces of the plate. So these stresses are determined by integrating the equilibrium equations of 3D elasticity with respect to thickness coordinate as

$$\tau_{xz} = -\int_{-h/2}^{z}\left(\frac{\partial\sigma_x}{\partial x}+\frac{\partial\tau_{xy}}{\partial y}\right)dz + C_1(x,y) \tag{17a}$$

$$\tau_{yz} = -\int_{-h/2}^{z}\left(\frac{\partial\tau_{xy}}{\partial x}+\frac{\partial\sigma_y}{\partial y}\right)dz + C_2(x,y) \tag{17b}$$

where $C_i$($i$=1, 2) are constants and determined by the following boundary conditions at the upper and lower surfaces of the plate

$$\tau_{xz}\big|_{z=\pm h/2} = 0, \quad \tau_{yz}\big|_{z=\pm h/2} = 0 \tag{18}$$

## 3. Analytical solution for rectangular FG plates

The Navier solution method is used to determine the analytical solutions for which the displacement variables are expressed as product of arbitrary parameters and known trigonometric functions to respect the governing equations and boundary conditions.

$$\begin{Bmatrix} u_0 \\ v_0 \\ w_0 \\ \theta \\ \varphi \end{Bmatrix} = \sum_{m=1}^{\infty}\sum_{n=1}^{\infty}\begin{Bmatrix} U_{mn}e^{i\omega t}\cos(\alpha x)\sin(\beta y) \\ V_{mn}e^{i\omega t}\sin(\alpha x)\cos(\beta y) \\ W_{mn}e^{i\omega t}\sin(\alpha x)\sin(\beta y) \\ X_{mn}e^{i\omega t}\sin(\alpha x)\sin(\beta y) \\ \Phi_{mn}e^{i\omega t}\sin(\alpha x)\sin(\beta y) \end{Bmatrix} \tag{19}$$

where ($U_{mn}$, $V_{mn}$, $W_{mn}$, $X_{mn}$, $\Phi_{mn}$) are unknown functions to be determined and $\omega$ is the natural frequency. $\alpha$ and $\beta$ are expressed as

$$\alpha = m\pi/a \text{ and } \beta = n\pi/b \tag{20}$$

The transverse distributed load $q(x,y)$ is also expanded double Fourier series as

$$q(x,y) = \sum_{m=1}^{\infty}\sum_{n=1}^{\infty} q_{mn}\sin\left(\frac{m\pi}{a}x\right)\sin\left(\frac{n\pi}{b}y\right) \tag{21}$$

The coefficients $q_{mn}$ are given below for some general loadings:

• For uniformly distributed load

$$q_{mn} = \begin{cases} \dfrac{16q_0}{mn\pi^2}, & m,n = 1,3,5,..... \\ 0 & m,n = 2,4,6,..... \end{cases} \tag{22}$$

• For uniformly distributed load

$$q_{mn} = q_0 \tag{23}$$

in which $q_0$ is the intensity of the load.

Substituting the stress and moment resultants defined in Eq. (15) into equations of motion (14) we get below closed-form solutions of static and free vibration problems of FG plate

$$\left(\begin{bmatrix} S_{11} & S_{12} & S_{13} & S_{14} & S_{15} \\ S_{12} & S_{22} & S_{23} & S_{24} & S_{25} \\ S_{13} & S_{23} & S_{33} & S_{34} & S_{35} \\ S_{14} & S_{24} & S_{34} & S_{44} & S_{45} \\ S_{15} & S_{25} & S_{35} & S_{45} & S_{55} \end{bmatrix} - \omega^2\begin{bmatrix} m_{11} & 0 & m_{13} & m_{14} & 0 \\ 0 & m_{22} & m_{23} & m_{24} & 0 \\ m_{13} & m_{23} & m_{33} & m_{34} & m_{35} \\ m_{14} & m_{24} & m_{34} & m_{44} & 0 \\ 0 & 0 & m_{35} & 0 & m_{55} \end{bmatrix}\right)\begin{Bmatrix} U_{mn} \\ V_{mn} \\ W_{mn} \\ X_{mn} \\ \Phi_{mn} \end{Bmatrix} = \begin{Bmatrix} 0 \\ 0 \\ q_{mn} \\ 0 \\ 0 \end{Bmatrix} \tag{24}$$

in which

$$\begin{aligned}
&S_{11} = \alpha^2 B_{11} + \beta^2 A_{66} \\
&S_{12} = \alpha\beta(A_{12} + A_{66}) \\
&S_{13} = -\alpha^3 B_{11} - \alpha\beta^2(B_{12} + 2B_{66}) \\
&S_{14} = -\alpha(k_1 B^s_{11} + k_2 B^s_{12}) + \alpha\beta^2 B^s_{66}(k_1 A' + k_2 B') \\
&S_{15} = \alpha X_{13} \\
&S_{22} = \alpha^2 A_{66} + \beta^2 A_{22} \\
&S_{23} = -\beta^3 B_{22} - \alpha^2\beta(B_{12} + 2B_{66}) \\
&S_{24} = -\beta(k_1 B^s_{12} + k_2 B^s_{22}) + \alpha^2\beta(k_1 A' + k_2 B')B^s_{66} \\
&S_{25} = -\beta X_{23} \\
&S_{33} = \alpha^4 D_{11} + \beta^4 D_{22} + 2\alpha^2\beta^2(D_{12} + 2D_{66}) \quad S_{33} = \alpha^4 D_{11} + \beta^4 D_{22} + 2\alpha^2\beta^2(D_{12} + 2D_{66}) \\
&S_{34} = \alpha^2 k_1 D^s_{11} + (k_2\alpha^2 + k_1\beta^2)D^s_{12} + \beta^2 k_2 D^s_{22} - 2\alpha^2\beta^2(k_1 A' + k_2 B')D^s_{66} \\
&S_{35} = \alpha^2 Y_{13} + \beta^2 Y_{23} \\
&S_{44} = k_1^2 H^s_{11} + k_2^2 H^s_{22} + 2k_1 k_2 H^s_{12} + \alpha^2\beta^2(k_1 A' + k_2 B')^2 H^s_{66} + \alpha^2(k_1 A')^2 A^s_{55} + \beta^2(k_2 B')^2 A^s_{44} \\
&S_{45} = k_1 Y^s_{13} + k_2 Y^s_{23} + \alpha^2 k_1 A' A^s_{55} + \beta^2 k_2 B' A^s_{44} \\
&S_{55} = \alpha^2 A^s_{55} + \beta^2 A^s_{44} + Z_{33} \\
&m_{11} = I_0 \\
&m_{13} = -\alpha I_1 \\
&m_{14} = k_1 A' \alpha J_1 \\
&m_{22} = I_0 \\
&m_{23} = -\beta I_1 \\
&m_{24} = k_2 B' \beta J_1 \\
&m_{33} = I_0 + I_2(\alpha^2 + \beta^2) \\
&m_{34} = J_2(k_1 + k_2) \\
&m_{35} = J_0 \\
&m_{44} = K_2((k_1 A')^2\alpha^2 + (k_2 B')^2\beta^2) \\
&m_{55} = K_0
\end{aligned} \tag{25}$$

## 4. Numerical results

In order to demonstrate the accuracy of the proposed theory in investigating the bending and dynamic responses of simply supported FG plates, numerical examples are presented and compared with the results of various 3D, quasi-3D and 2D shear deformation theories.

### *4.1 Bending analysis*

#### *4.1.1 Functionally graded plates*

In this section, the computed stress and displacements of FG plates which are graded from the lower to the upper surface according to Eq. (1) are provided and compared with the results of different HSDTs. The material properties of FG plates are listed in Table 1.

Tables 2 and 3 show the non-dimensional displacement and stresses of an $Al/Al_2O_3$ FG square plate under uniformly and sinusoidal distributed loads for various values of the

Table 1 Material properties used in the FG plates

| Material | Properties | | |
|---|---|---|---|
| | $E$(GPa) | $v$ | $p$(kg/m$^3$) |
| Aluminum (Al) | 70 | 0.3 | 2702 |
| Alumina ($Al_2O_3$) | 380 | 0.3 | 3800 |
| Zirconia ($ZrO_2$) | 200 | 0.3 | 5700 |

Table 2 The non-dimensional displacement and stress components of an $Al/Al_2O_3$ FG square plate subjected to uniformly distributed load ($a/h$=10)

| $k$ | Theory | $\varepsilon_z$ | $\bar{w}(0)$ | $\bar{\sigma}_x\left(\frac{h}{2}\right)$ | $\bar{\sigma}_y\left(\frac{h}{3}\right)$ | $\bar{\tau}_{xz}(0)$ | $\bar{\tau}_{yz}\left(\frac{h}{6}\right)$ | $\bar{\tau}_{xy}\left(-\frac{h}{3}\right)$ |
|---|---|---|---|---|---|---|---|---|
| 0 | Akavci and Tanrikulu (2015) | = 0 | 0.4665 | 2.8909 | 1.9103 | 0.4988 | 0.4363 | 1.2857 |
| | Present | = 0 | 0.4665 | 2.8913 | 1.9102 | 0.5043 | 0.4367 | 1.2855 |
| | Akavci and Tanrikulu (2015) | ≠ 0 | 0.4635 | 2.9981 | 1.8925 | 0.4782 | 0.4315 | 1.2578 |
| | Present | ≠ 0 | 0.4637 | 2.9919 | 1.8932 | 0.4791 | 0.4317 | 1.2585 |
| 1 | Akavci and Tanrikulu (2015) | = 0 | 0.9288 | 4.4707 | 2.1693 | 0.4988 | 0.5364 | 1.1141 |
| | Present | = 0 | 0.9287 | 4.4713 | 2.1692 | 0.5043 | 0.5370 | 1.1141 |
| | Akavci and Tanrikulu (2015) | ≠ 0 | 0.8977 | 4.6110 | 2.0822 | 0.4782 | 0.5119 | 1.0211 |
| | Present | ≠ 0 | 0.8980 | 4.6005 | 2.0832 | 0.4791 | 0.5121 | 1.0225 |
| 2 | Akavci and Tanrikulu (2015) | = 0 | 1.1940 | 5.2248 | 2.0342 | 0.4581 | 0.5643 | 0.9909 |
| | Present | = 0 | 1.1940 | 5.2256 | 2.0340 | 0.4637 | 0.5657 | 0.9908 |
| | Akavci and Tanrikulu (2015) | ≠ 0 | 1.1376 | 5.3825 | 1.9257 | 0.4524 | 0.5081 | 0.8921 |
| | Present | ≠ 0 | 1.1380 | 5.3726 | 1.9281 | 0.4532 | 0.5082 | 0.8926 |
| 4 | Akavci and Tanrikulu (2015) | = 0 | 1.3888 | 5.8855 | 1.7205 | 0.4090 | 0.5253 | 1.0305 |
| | Present | = 0 | 1.3890 | 5.8866 | 1.7202 | 0.4151 | 0.5278 | 1.0303 |
| | Akavci and Tanrikulu (2015) | ≠ 0 | 1.3259 | 6.0382 | 1.6062 | 0.4358 | 0.4804 | 0.9274 |
| | Present | ≠ 0 | 1.3262 | 6.0301 | 1.6101 | 0.4365 | 0.4806 | 0.9279 |
| 10 | Akavci and Tanrikulu (2015) | = 0 | 1.5875 | 7.3617 | 1.2828 | 0.4436 | 0.4159 | 1.0705 |
| | Present | = 0 | 1.5875 | 7.3628 | 1.2825 | 0.4495 | 0.4174 | 1.0703 |
| | Akavci and Tanrikulu (2015) | ≠ 0 | 1.5453 | 7.5123 | 1.2016 | 0.4332 | 0.4561 | 0.9860 |
| | Present | ≠ 0 | 1.5454 | 7.5064 | 1.2059 | 0.4339 | 0.4562 | 0.9862 |

power-law index. The non-dimensional displacement and stress components for these Tables are given in Eq. (25). Table 2 provides the computed results of non-dimensional displacement and stress components of the square FG plate subjected to uniform load as compared with those given by the quasi-3D and 2D shear deformation theories by Akavci and Tanrikulu (2015). It can be observed from the table that the proposed 2D and 3D theory results are in excellent agreement with those of Akavci and Tanrikulu (2015). This table also demonstrates that, the deflection $\bar{w}$ and in-plane stresses $\bar{\sigma}_x$ and $\bar{\sigma}_y$ increase and the shear stresses $\bar{\tau}_{xz}$ and $\bar{\tau}_{xy}$ diminish with the increasing value of material index $k$. Table 3 provides the non-dimensional in-plane stresses $\bar{\sigma}_x$ and non-dimensional deflection $\bar{w}$ of a square plate for different $a/h$ ratios. The obtained results are compared with the different quasi-3D HSDTs of Carrera *et al.* (2011) Neves *et al.* (2012a, b), Hebali *et al.* (2014) and Akavci and Tanrikulu (2015) that include both transverse shear and normal deformations. The proposed quasi-3D results agree very well with those provided by other models.

Table 3 Non-dimensional displacement and stress of an $Al/Al_2O_3$ FG square plate subjected to sinusoidal load

| $k$ | Theory | $\varepsilon_z$ | $\bar{\sigma}_x(0)$ | | | $\bar{w}(0)$ | | |
|---|---|---|---|---|---|---|---|---|
| | | | $a/h$=4 | $a/h$=10 | $a/h$=100 | $a/h$=4 | $a/h$=10 | $a/h$=100 |
| 1 | Carrera *et al.* (2011) | ≠ 0 | 0.6221 | 1.5064 | 14.9690 | 0.7171 | 0.5875 | 0.5625 |
| | Neves *et al.* (2012a) | ≠ 0 | 0.5925 | 1.4945 | 14.9690 | 0.6997 | 0.5845 | 0.5624 |
| | Neves *et al.* (2012b) | ≠ 0 | 0.5910 | 1.4917 | 14.9440 | 0.7020 | 0.5868 | 0.5648 |
| | Hebali *et al.* (2014) | ≠ 0 | 0.5952 | 1.4954 | 14.9630 | 0.6910 | 0.5686 | 0.5452 |
| | Akavci and Tanrikulu (2015) | = 0 | 0.5806 | 1.4895 | 14.9670 | 0.7282 | 0.5889 | 0.5625 |
| | Present | = 0 | 0.5808 | 1.4896 | 14.9675 | 0.7283 | 0.5889 | 0.5625 |
| | Akavci and Tanrikulu (2015) | ≠ 0 | 0.5754 | 1.4322 | 14.3060 | 0.6908 | 0.5691 | 0.5457 |
| | Present | ≠ 0 | 0.5758 | 1.4330 | 14.3135 | 0.6910 | 0.5692 | 0.5459 |
| 4 | Carrera *et al.* (2011) | ≠ 0 | 0.4877 | 1.1971 | 11.9230 | 1.1585 | 0.8821 | 0.8286 |
| | Neves *et al.* (2012a) | ≠ 0 | 0.4404 | 1.1783 | 11.9320 | 1.1178 | 0.8750 | 0.8286 |
| | Neves *et al.* (2012b) | ≠ 0 | 0.4340 | 1.1593 | 11.7380 | 1.1095 | 0.8698 | 0.8241 |
| | Hebali *et al.* (2014) | ≠ 0 | 0.4507 | 1.1779 | 11.8710 | 1.0964 | 0.8413 | 0.7926 |
| | Akavci and Tanrikulu (2015) | = 0 | 0.4431 | 1.1787 | 11.9200 | 1.1613 | 0.8818 | 0.8287 |
| | Present | = 0 | 0.4437 | 1.1789 | 11.9209 | 1.1609 | 0.8817 | 0.8287 |
| | Akavci and Tanrikulu (2015) | ≠ 0 | 0.4247 | 1.1017 | 11.0880 | 1.0983 | 0.8417 | 0.7925 |
| | Present | ≠ 0 | 0.4260 | 1.1045 | 11.1152 | 1.0982 | 0.8419 | 0.7928 |
| 10 | Carrera *et al.* (2011) | ≠ 0 | 0.3965 | 0.8965 | 8.9077 | 1.3745 | 1.0072 | 0.9361 |
| | Neves *et al.* (2012a) | ≠ 0 | 0.3227 | 1.1783 | 11.9320 | 1.3490 | 0.8750 | 0.8286 |
| | Neves *et al.* (2012b) | ≠ 0 | 0.3108 | 0.8467 | 8.6013 | 1.3327 | 0.9886 | 0.9228 |
| | Hebali *et al.* (2014) | ≠ 0 | 0.3325 | 0.8889 | 8.9977 | 1.3333 | 0.9791 | 0.9114 |
| | Akavci and Tanrikulu (2015) | = 0 | 0.3242 | 0.8778 | 8.9059 | 1.3917 | 1.0089 | 0.9362 |
| | Present | = 0 | 0.3248 | 0.8780 | 8.9059 | 1.3915 | 1.0088 | 0.9362 |
| | Akavci and Tanrikulu (2015) | ≠ 0 | 0.3095 | 0.8229 | 8.3185 | 1.3352 | 0.9818 | 0.9141 |
| | Present | ≠ 0 | 0.3109 | 0.8259 | 8.3473 | 1.3353 | 0.9819 | 0.9141 |

$$\bar{w}=\frac{10h^3E_c}{a^4q_0}w\left(\frac{a}{2},\frac{b}{2},z\right),\ \bar{\sigma}_x=\frac{h}{aq_0}\sigma_x\left(\frac{a}{2},\frac{b}{2},z\right),\ \bar{\sigma}_y=\frac{h}{aq_0}\sigma_y\left(\frac{a}{2},\frac{b}{2},z\right),$$
$$\bar{\tau}_{xy}=\frac{h}{aq_0}\tau_{xy}(0,0,z),\ \bar{\tau}_{xz}=\frac{h}{aq_0}\tau_{xz}\left(0,\frac{b}{2},z\right),\ \bar{\tau}_{yz}=\frac{h}{aq_0}\tau_{yz}\left(\frac{a}{2},0,z\right) \tag{26}$$

Fig. 2 presents the stress and displacement variations through the thickness of $Al/Al_2O_3$ FG square plate subjected to sinusoidal load. The non-dimensional quantities presented in Fig. 2 are given in Eq. (26). The results are shown as compared with the quasi-3D and 2D shear deformation theories of Akavci and Tanrikulu (2015) for various values of material index $k$. According to Fig. 2, the results are in excellent agreement with those computed

using of the quasi-3D and 2D shear deformation theories of Akavci and Tanrikulu (2015). It is important to indicate that, the through the thickness variations of in-plane stresses $\bar{\sigma}_x$ and $\bar{\tau}_{xy}$ are linear for homogeneous plate while it is parabolic for FG plates.

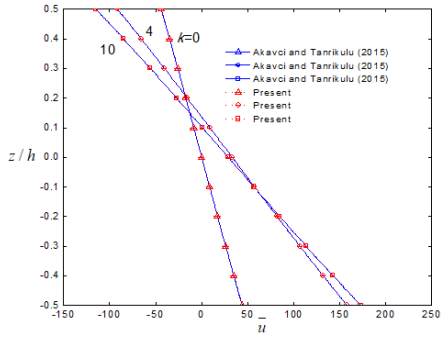


(a)

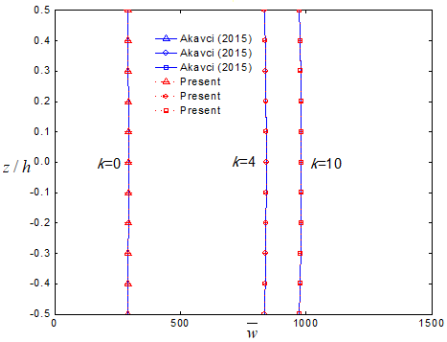


(b)

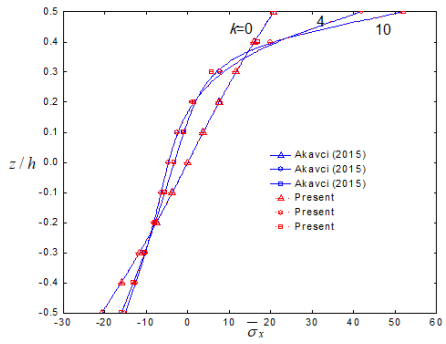


(c)

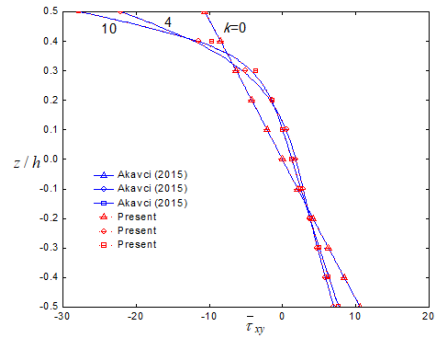


(d)

Fig. 2 The distributions of the non-dimensional displacement and stresses of square FG plate ($a/h$=10), (a) In-plane displacement ( $\bar{u}$ ), (b) Transverse displacement ( $\bar{w}$ ), (c) axial stress ( $\bar{\sigma}_x$ ), (d) in-plane shear stress ( $\bar{\tau}_{xy}$ ) and (e) transverse shear stress ( $\bar{\tau}_{xz}$ )

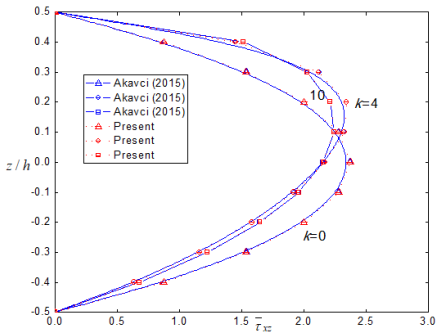


(e)

Fig. 2 Continued

Table 4 Non-dimensional deflection $\bar{w}(0)=\frac{10h^3E_0}{a^4q_0}w\left(\frac{a}{2},\frac{b}{2},0\right)$ of EGM plates subjected to sinusoidal distributed load ($a/h$=2)

| $b/a$ | Theory | $\varepsilon_z$ | $p$ | | | | | |
|---|---|---|---|---|---|---|---|---|
| | | | 0.1 | 0.3 | 0.5 | 0.7 | 1 | 1.5 |
| 1 | Zenkour (2007) | ≠ 0 | 0.5769 | 0.5247 | 0.4766 | 0.4324 | 0.3726 | 0.2890 |
| | Zenkour (2007) | = 0 | 0.5730 | 0.5180 | 0.4678 | 0.4221 | 0.3611 | 0.2771 |
| | Mantari and Soares (2013) | ≠ 0 | 0.5778 | 0.5224 | 0.4717 | 0.4256 | 0.3648 | 0.2793 |
| | Mantari and Soares (2013) | = 0 | 0.6362 | 0.5751 | 0.5194 | 0.4687 | 0.4017 | 0.3079 |
| | Akavci and Tanrikulu (2015) | = 0 | 0.6351 | 0.5741 | 0.5185 | 0.4679 | 0.4004 | 0.3075 |
| | Present | = 0 | 0.6355 | 0.5745 | 0.5189 | 0.4683 | 0.4007 | 0.3077 |
| | Akavci and Tanrikulu (2015) | ≠ 0 | 0.5750 | 0.5198 | 0.4694 | 0.4236 | 0.3624 | 0.2780 |
| | Present | ≠ 0 | 0.5758 | 0.5205 | 0.4701 | 0.4242 | 0.3629 | 0.2784 |
| 2 | Zenkour (2007) | ≠ 0 | 1.1944 | 1.0859 | 0.9864 | 0.8952 | 0.7726 | 0.6017 |
| | Zenkour (2007) | = 0 | 1.1879 | 1.0739 | 0.9700 | 0.8754 | 0.7493 | 0.5757 |
| | Mantari and Soares (2013) | ≠ 0 | 1.1940 | 1.0794 | 0.9750 | 0.8799 | 0.7537 | 0.5786 |
| | Mantari and Soares (2013) | = 0 | 1.2776 | 1.1553 | 1.0441 | 0.9430 | 0.8092 | 0.6237 |
| | Akavci and Tanrikulu (2015) | = 0 | 1.2763 | 1.1541 | 1.0431 | 0.9422 | 0.8079 | 0.6234 |
| | Present | = 0 | 1.2768 | 1.1546 | 1.0435 | 0.9426 | 0.8082 | 0.6236 |
| | Akavci and Tanrikulu (2015) | ≠ 0 | 1.1938 | 1.0765 | 0.9723 | 0.8775 | 0.7511 | 0.5771 |
| | Present | ≠ 0 | 1.1917 | 1.0774 | 0.9731 | 0.8782 | 0.7517 | 0.5775 |
| 3 | Zenkour (2007) | ≠ 0 | 1.4429 | 1.3116 | 1.9112 | 1.0811 | 0.9333 | 0.7275 |
| | Zenkour (2007) | = 0 | 1.4354 | 1.2977 | 1.1722 | 1.0579 | 0.9056 | 0.6961 |
| | Mantari and Soares (2013) | ≠ 0 | 1.4421 | 1.3037 | 1.1776 | 1.0627 | 0.9104 | 0.6992 |
| | Mantari and Soares (2013) | = 0 | 1.5340 | 1.3873 | 1.2540 | 1.1329 | 0.9725 | 0.7506 |
| | Akavci and Tanrikulu (2015) | = 0 | 1.5327 | 1.3861 | 1.2530 | 1.1320 | 0.9712 | 0.7503 |
| | Present | = 0 | 1.5332 | 1.3866 | 1.2534 | 1.1324 | 0.9715 | 0.7504 |
| | Akavci and Tanrikulu (2015) | ≠ 0 | 1.4386 | 1.3005 | 1.1748 | 1.0602 | 0.9076 | 0.6976 |
| | Present | ≠ 0 | 1.4396 | 1.3015 | 1.1756 | 1.0610 | 0.9082 | 0.6981 |

### *4.1.2 Exponentially graded plates*

In this section, the exponential function employed to define the material properties of the EGM plate is given in Eq. (2). The non-dimensional stress and displacements of the E-FGM plate are compared with the results of different HSDTs for different loadings.

The non-dimensional displacements and stresses are given in Tables 4-6 for different values of aspect ratio $b/a$,

Table 5 Non-dimensional stress $\bar{\sigma}_x\left(\frac{h}{2}\right)=\frac{h^2}{a^2 q_0}\sigma_x\left(\frac{a}{2},\frac{b}{2},\frac{h}{2}\right)$ of EGM plates subjected to sinusoidal distributed load ($a/h$=10)

| $b/a$ | Theory | $\varepsilon_z$ | $p$ | | | | | | | | |
|---|---|---|---|---|---|---|---|---|---|---|---|
| | | | 0.1 | 0.3 | 0.5 | 0.7 | 1 | 1.5 | 2 | 2.5 | 3 |
| 1 | Mantari and Soares (2013) | ≠ 0 | 0.2196 | 0.2345 | 0.2503 | 0.2671 | 0.2944 | 0.3460 | 0.4065 | 0.4775 | 0.5603 |
| | Mantari and Soares (2013) | = 0 | 0.2062 | 0.2204 | 0.2355 | 0.2515 | 0.2774 | 0.3264 | 0.3835 | 0.4502 | 0.5278 |
| | Akavci and Tanrikulu (2015) | = 0 | 0.2063 | 0.2205 | 0.2356 | 0.2516 | 0.2776 | 0.3266 | 0.3838 | 0.4504 | 0.5281 |
| | Present | = 0 | 0.2063 | 0.2205 | 0.2355 | 0.2516 | 0.2775 | 0.3265 | 0.3837 | 0.4504 | 0.5279 |
| | Akavci and Tanrikulu (2015) | ≠ 0 | 0.2142 | 0.2285 | 0.2438 | 0.2601 | 0.2866 | 0.3370 | 0.3964 | 0.4664 | 0.5485 |
| | Present | ≠ 0 | 0.2137 | 0.2280 | 0.2433 | 0.2595 | 0.2860 | 0.3363 | 0.3957 | 0.4657 | 0.5478 |
| 2 | Mantari and Soares (2013) | ≠ 0 | 0.4552 | 0.4867 | 0.5200 | 0.5554 | 0.6126 | 0.7201 | 0.8449 | 0.9898 | 1.1580 |
| | Mantari and Soares (2013) | = 0 | 0.4350 | 0.4649 | 0.4966 | 0.5303 | 0.5850 | 0.6881 | 0.8085 | 0.9490 | 1.1125 |
| | Akavci and Tanrikulu (2015) | = 0 | 0.4351 | 0.4650 | 0.4968 | 0.5305 | 0.5852 | 0.6884 | 0.8088 | 0.9493 | 1.1129 |
| | Present | = 0 | 0.4351 | 0.4650 | 0.4967 | 0.5305 | 0.5851 | 0.6883 | 0.8087 | 0.9492 | 1.1128 |
| | Akavci and Tanrikulu (2015) | ≠ 0 | 0.4466 | 0.4773 | 0.5098 | 0.5443 | 0.6002 | 0.7058 | 0.8289 | 0.9725 | 1.1397 |
| | Present | ≠ 0 | 0.4459 | 0.4765 | 0.5090 | 0.5435 | 0.5993 | 0.7048 | 0.8278 | 0.8278 | 1.1388 |
| 3 | Mantari and Soares (2013) | ≠ 0 | 0.5514 | 0.5896 | 0.6302 | 0.6733 | 0.7427 | 0.8730 | 1.0240 | 1.1990 | 1.4017 |
| | Mantari and Soares (2013) | = 0 | 0.5288 | 0.5651 | 0.6037 | 0.6447 | 0.7112 | 0.8365 | 0.9828 | 1.1536 | 1.3523 |
| | Akavci and Tanrikulu (2015) | = 0 | 0.5290 | 0.5653 | 0.6039 | 0.6449 | 0.7114 | 0.8368 | 0.9832 | 1.1540 | 1.3528 |
| | Present | = 0 | 0.5289 | 0.5652 | 0.6038 | 0.6449 | 0.7113 | 0.8367 | 0.9831 | 1.1538 | 1.3527 |
| | Akavci and Tanrikulu (2015) | ≠ 0 | 0.5418 | 0.5791 | 0.6187 | 0.6608 | 0.7289 | 0.8570 | 1.0061 | 1.1797 | 1.3813 |
| | Present | ≠ 0 | 0.5410 | 0.5783 | 0.6179 | 0.6599 | 0.7279 | 0.8559 | 1.0050 | 1.1786 | 1.3803 |

thickness ratio $a/h$ and exponent value $p$. Table 4 shows the central deflections of the very thick E-FGM plates. The computed results are compared with the quasi-3D sinusoidal and exact 3D elasticity theories of Zenkour (2007), 2D and quasi-3D trigonometric models of Mantari and Soares (2013) and the quasi-3D and 2D shear deformation theories by Akavci and Tanrikulu (2015). Since the presented and other quasi-3D models introduce the thickness-stretching influence, the results are close to each other. Meanwhile, 2D HSDTs which do not introduce the thickness stretching influence overestimate the results. In Tables 5 and 6, the computed non-dimensional stresses are

Table 6 Non-dimensional stress $\bar{\tau}_{xz}(0)=\frac{h}{a q_0}\tau_{xz}\left(0,\frac{b}{2},0\right)$ of EGM plates subjected to sinusoidal distributed load ($a/h$=10)

| $b/a$ | Theory | $\varepsilon_z$ | $p$ | | | | | | | | |
|---|---|---|---|---|---|---|---|---|---|---|---|
| | | | 0.1 | 0.3 | 0.5 | 0.7 | 1 | 1.5 | 2 | 2.5 | 3 |
| 1 | Mantari and Soares (2013) | ≠ 0 | 0.2454 | 0.2450 | 0.2442 | 0.2430 | 0.2405 | 0.2344 | 0.2263 | 0.2162 | 0.2045 |
| | Mantari and Soares (2013) | = 0 | 0.2380 | 0.2376 | 0.2368 | 0.2356 | 0.2330 | 0.2268 | 0.2185 | 0.2094 | 0.1985 |
| | Akavci and Tanrikulu (2015) | = 0 | 0.2434 | 0.2430 | 0.2422 | 0.2410 | 0.2385 | 0.2324 | 0.2242 | 0.2140 | 0.2023 |
| | Present | = 0 | 0.2416 | 0.2412 | 0.2404 | 0.2392 | 0.2366 | 0.2305 | 0.2222 | 0.2121 | 0.2003 |
| | Akavci and Tanrikulu (2015) | ≠ 0 | 0.2367 | 0.2364 | 0.2359 | 0.2353 | 0.2338 | 0.2300 | 0.2249 | 0.2182 | 0.2102 |
| | Present | ≠ 0 | 0.2371 | 0.2369 | 0.2364 | 0.2357 | 0.2342 | 0.2304 | 0.2252 | 0.2186 | 0.2105 |
| 2 | Mantari and Soares (2013) | ≠ 0 | 0.3927 | 0.3921 | 0.3908 | 0.3889 | 0.3849 | 0.3752 | 0.3621 | 0.3460 | 0.3273 |
| | Mantari and Soares (2013) | = 0 | 0.3810 | 0.3803 | 0.3790 | 0.3770 | 0.3730 | 0.3630 | 0.3497 | 0.3344 | 0.3165 |
| | Akavci and Tanrikulu (2015) | = 0 | 0.3896 | 0.3889 | 0.3877 | 0.3857 | 0.3817 | 0.3719 | 0.3588 | 0.3425 | 0.3237 |
| | Present | = 0 | 0.3867 | 0.3860 | 0.3847 | 0.3828 | 0.3787 | 0.3689 | 0.3557 | 0.3394 | 0.3206 |
| | Akavci and Tanrikulu (2015) | ≠ 0 | 0.3790 | 0.3787 | 0.3779 | 0.3768 | 0.3744 | 0.3684 | 0.3602 | 0.3496 | 0.3368 |
| | Present | ≠ 0 | 0.3797 | 0.3793 | 0.3786 | 0.3774 | 0.3750 | 0.3691 | 0.3608 | 0.3501 | 0.3373 |
| 3 | Mantari and Soares (2013) | ≠ 0 | 0.4418 | 0.4411 | 0.4396 | 0.4375 | 0.4330 | 0.4221 | 0.4074 | 0.3893 | 0.3683 |
| | Mantari and Soares (2013) | = 0 | 0.4286 | 0.4279 | 0.4264 | 0.4242 | 0.4196 | 0.4084 | 0.3934 | 0.3761 | 0.3558 |
| | Akavci and Tanrikulu (2015) | = 0 | 0.4383 | 0.4376 | 0.4361 | 0.4340 | 0.4294 | 0.4185 | 0.4036 | 0.3854 | 0.3642 |
| | Present | = 0 | 0.4350 | 0.4343 | 0.4328 | 0.4307 | 0.4261 | 0.4151 | 0.4002 | 0.3819 | 0.3607 |
| | Akavci and Tanrikulu (2015) | ≠ 0 | 0.4265 | 0.4261 | 0.4252 | 0.4239 | 0.4212 | 0.4146 | 0.4053 | 0.3934 | 0.3789 |
| | Present | ≠ 0 | 0.4273 | 0.4268 | 0.4260 | 0.4247 | 0.4220 | 0.4153 | 0.4059 | 0.3940 | 0.3795 |

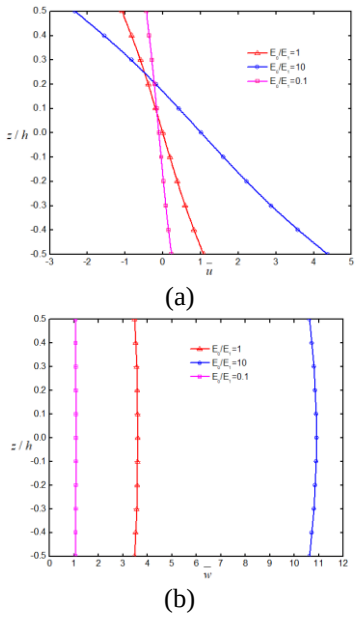


(a)

(b)

Fig. 3 The distributions of the non-dimensional displacement and stresses of square EGM plate subjected to sinusoidal load versus $E_0/E_1$ rations ($a/h$=4), (a) In-plane displacement ($\bar{u}$), (b) Transverse displacement ($\bar{w}$), (c) axial stress ($\bar{\sigma}_x$), (d) in-plane shear stress ($\bar{\tau}_{xy}$) and (e) transverse shear stress ($\bar{\tau}_{xz}$)

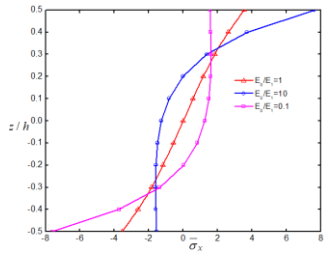


(c)

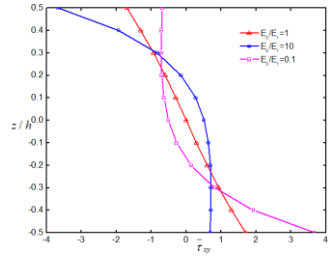


(d)

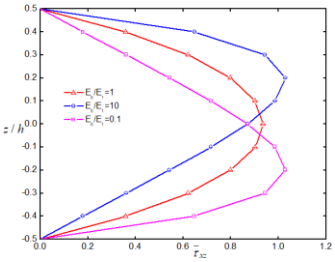


(e)

Fig. 3 Continued

Table 7 Non-dimensional central displacement $\bar{w}(0)=G(h)w/hq_0$ and in-plane normal stress $\bar{\sigma}_x(0)=\sigma_x(0)/q_0$ of EGM plates subjected to uniformly distributed load

| $h/a$ | Quantity | Theory | $E_0/E_1$ | | | | |
|---|---|---|---|---|---|---|---|
| | | | 0.1 | 0.5 | 1 | 2 | 10 |
| 0.2 | $\bar{w}$ | BEM (Vaghefi *et al.* 2010) | 4.0916 | 8.9751 | 12.5990 | 17.6640 | 39.0600 |
| | | FEM (Vaghefi *et al.* 2010) | 4.1215 | 9.0047 | 12.6130 | 17.7110 | 39.1550 |
| | | Akavci and Tanrikulu (2015): $\varepsilon_z\neq 0$ | 3.8333 | 8.8724 | 12.5970 | 17.7440 | 38.3330 |
| | | Present: $\varepsilon_z\neq 0$ | 3.8345 | 8.8756 | 12.6025 | 17.7511 | 38.3451 |
| | $\bar{\sigma}_x$ | BEM (Vaghefi *et al.* 2010) | -15.356 | -9.2902 | -7.4462 | -5.9410 | -3.4665 |
| | | FEM (Vaghefi *et al.* 2010) | -15.403 | -9.2995 | -7.4588 | -5.9591 | -3.4805 |
| | | Akavci and Tanrikulu (2015): $\varepsilon_z\neq 0$ | -16.3220 | -9.6545 | -7.6944 | -6.1109 | -3.4530 |
| | | Present: $\varepsilon_z\neq 0$ | -16.2898 | -9.6313 | -7.6770 | -6.0994 | -3.4504 |
| 0.3 | $\bar{w}$ | BEM (Vaghefi *et al.* 2010) | 0.9707 | 2.1378 | 2.9853 | 4.1208 | 8.7134 |
| | | FEM (Vaghefi *et al.* 2010) | 0.9732 | 2.1407 | 2.9792 | 4.1333 | 8.7293 |
| | | Zhang *et al.* (2014) | 0.9735 | 2.1405 | 2.9795 | 4.1332 | 8.7343 |
| | | Akavci and Tanrikulu (2015): $\varepsilon_z\neq 0$ | 0.8923 | 2.0834 | 2.9602 | 4.1669 | 8.9229 |
| | | Present: $\varepsilon_z\neq 0$ | 0.8925 | 2.0843 | 2.9615 | 4.1685 | 8.9253 |
| | $\bar{\sigma}_x$ | BEM (Vaghefi *et al.* 2010) | -7.223 | -4.3084 | -3.4496 | -2.7499 | -1.6449 |
| | | FEM (Vaghefi *et al.* 2010) | -7.2639 | -4.3378 | -3.4681 | -2.7673 | -1.6499 |
| | | Zhang *et al.* (2014) | -7.1493 | -4.3227 | -3.4710 | -2.7853 | -1.6759 |
| | | Akavci and Tanrikulu (2015): $\varepsilon_z\neq 0$ | -7.6576 | -4.5062 | -3.5748 | -2.8235 | -1.5731 |
| | | Present: $\varepsilon_z\neq 0$ | -7.6386 | -4.4941 | -3.5659 | -2.8175 | -1.5715 |

provided as compared with the quasi-3D and 2D hyperbolic theories by Akavci and Tanrikulu (2015) and 2D and quasi-3D trigonometric theories of Mantari and Soares (2013). It is evident from the examination of the tables that the present results are in an excellent agreement with the quasi-3D solutions of (Akavci and Tanrikulu 2015, Mantari and Soares 2013). Tables 4-6 demonstrate also that deflection $\bar{w}$ and transverse shear stress $\bar{\tau}_{xz}$ diminish and in plane stress $\bar{\sigma}_x$ increases with the increase of exponent $p$.

Fig. 3 shows the variations of non-dimensional displacements and stresses within the thickness of an EGM plate subjected to sinusoidal loading for different $E_0/E_1$ ratios (where; $E_1=E(h)$ and $E_0=E(0)$). It can be seen from these results that the non-dimensional displacements increase with increasing $E_0/E_1$. In addition, it can be deduced that $E_0/E_1$ ratios affect considerably the non-dimensional stresses.

Table 7 shows the non-dimensional central deflections and stresses of the EGM plates for various values of $E_0/E_1$ ratios. The computed results are compared with the Finite Element Method (FEM) and Boundary Element Method (BEM) of Vaghefi *et al.* (2010), the exact 3D elasticity theory of Zhang *et al.* (2014) and the quasi-3D hyperbolic theory by Akavci and Tanrikulu (2015) and they match very well.

### *4.2 Free vibration*

In this section, numerical results are studied and discussed to check the accuracy of the proposed novel models in predicting the dynamic responses of simply supported FG plates.

In the first example, isotropic square plates are examined to verify the efficiency of the proposed theories. According to Eqs. (1)-(3), when the material index $p$, approaches zero or infinity, the plate is isotropic composed of fully ceramic or metal, respectively. In Table 8, the first eight non-dimensional natural frequencies are calculated and compared with the results given by the quasi-3D theories of Jha *et al.* (2013) and Hebali *et al.* (2014), exact 3D solution of Srinivas *et al.* (1970), the quasi-3D and 2D shear deformation theories by Akavci and Tanrikulu (2015) and first order shear deformation theory (FSDT) of Whitney and Pagano (1970). Table 8 proves that the computed results are in excellent agreement with those reported by the other quasi-3D theories of Jha *et al.* (2013), Hebali *et al.* (2014) and Akavci and Tanrikulu (2015) for all modes of vibration.

Table 8 Comparison of non-dimensional natural frequencies $\bar{\omega}=\omega h\sqrt{\rho/G}$ for isotropic square plate ($a/h$=10)

| Theory | $\varepsilon_z$ | Mode ($m$, $n$) | | | | | | | |
|---|---|---|---|---|---|---|---|---|---|
| | | (1.1) | (1.2) | (2.2) | (1.3) | (2.3) | (3.3) | (2.4) | (1.5) |
| Jha *et al.* (2013) | $\neq 0$ | 0.0932 | 0.2226 | 0.3421 | 0.4172 | 0.5240 | 0.6892 | 0.7515 | 0.9275 |
| Hebali *et al.* (2014) | $\neq 0$ | 0.0933 | 0.2228 | 0.3422 | 0.4173 | 0.5240 | 0.6890 | 0.7512 | 0.9268 |
| Srinivas *et al.* (1970) | $\neq 0$ | 0.0932 | 0.2226 | 0.3421 | 0.4171 | 0.5239 | 0.6889 | 0.7511 | 0.9268 |
| Whitney and Pagano (1970) | $=0$ | 0.0930 | 0.2220 | 0.3406 | 0.4149 | 0.5206 | 0.6834 | 0.7447 | 0.9174 |
| Akavci and Tanrikulu (2015) | $=0$ | 0.0930 | 0.2219 | 0.3407 | 0.4151 | 0.5209 | 0.6841 | 0.7455 | 0.9189 |

Table 8 Continued

| Theory | $\varepsilon_z$ | Mode ($m$, $n$) | | | | | | | |
|---|---|---|---|---|---|---|---|---|---|
| | | (1.1) | (1.2) | (2.2) | (1.3) | (2.3) | (3.3) | (2.4) | (1.5) |
| Present | = 0 | 0.0930 | 0.2220 | 0.3406 | 0.4151 | 0.5208 | 0.6840 | 0.7455 | 0.9188 |
| Akavci and Tanrikulu (2015) | ≠ 0 | 0.0932 | 0.2227 | 0.3424 | 0.4176 | 0.5247 | 0.6902 | 0.7526 | 0.9290 |
| Present | ≠ 0 | 0.0932 | 0.2227 | 0.3423 | 0.4175 | 0.5245 | 0.6899 | 0.7522 | 0.9285 |

Table 9 Comparison of the non-dimensional fundamental frequencies $\bar{\omega} = \omega h \sqrt{\frac{\rho_C}{E_C}}$ for Al/$Al_2O_3$ square plate

| $a/h$ | Theory | $\varepsilon_z$ | $k$ | | | | |
|---|---|---|---|---|---|---|---|
| | | | 0 | 0.5 | 1 | 4 | 10 |
| 2 | Zhu and Liew (2011) | = 0 | 0.9265 | 0.8060 | 0.7331 | 0.6112 | 0.5640 |
| | Matsunaga (2008) | ≠ 0 | 0.9400 | 0.8232 | 0.7477 | 0.5997 | 0.5460 |
| | Sheikholeslami and Saidi (2013) | ≠ 0 | 0.9400 | 0.8223 | 0.7475 | 0.5995 | 0.5461 |
| | Belabed *et al.* (2014) | ≠ 0 | 0.9414 | 0.8248 | 0.7516 | 0.6056 | 0.5495 |
| | Akavci and Tanrikulu (2015) | = 0 | 0.9303 | 0.8115 | 0.7360 | 0.5921 | 0.5413 |
| | Present | = 0 | 0.9301 | 0.8144 | 0.7416 | 0.5979 | 0.5436 |
| | Akavci and Tanrikulu (2015) | ≠ 0 | 0.9440 | 0.8269 | 0.7536 | 0.6063 | 0.5506 |
| | Present | ≠ 0 | 0.9434 | 0.8287 | 0.7574 | 0.6108 | 0.5522 |
| 5 | Zhu and Liew (2011) | = 0 | 0.2111 | 0.1804 | 0.1629 | 0.1395 | 0.1323 |
| | Benachour *et al.* (2011) | = 0 | 0.2112 | 0.1806 | 0.1628 | 0.1375 | 0.1300 |
| | Hosseini *et al.* (2011) | = 0 | 0.2113 | 0.1807 | 0.1631 | 0.1378 | 0.1301 |
| | Matsunaga (2008) | ≠ 0 | 0.2121 | 0.1819 | 0.1640 | 0.1383 | 0.1306 |
| | Sheikholeslami and Saidi (2013) | ≠ 0 | 0.2121 | 0.1818 | 0.1640 | 0.1382 | 0.1306 |
| | Belabed *et al.* (2014) | ≠ 0 | 0.2121 | 0.1819 | 0.1640 | 0.1383 | 0.1306 |
| | Akavci and Tanrikulu (2015) | = 0 | 0.2113 | 0.1807 | 0.1631 | 0.1378 | 0.1300 |
| | Present | = 0 | 0.2113 | 0.1808 | 0.1632 | 0.1379 | 0.1301 |
| | Akavci and Tanrikulu (2015) | ≠ 0 | 0.2124 | 0.1827 | 0.1661 | 0.1410 | 0.1319 |
| | Present | ≠ 0 | 0.2123 | 0.1827 | 0.1661 | 0.1411 | 0.1319 |
| 10 | Zhu and Liew (2011) | = 0 | 0.0576 | 0.0489 | 0.0441 | 0.0381 | 0.0365 |
| | Benachour *et al.* (2011) | = 0 | 0.0576 | 0.0490 | 0.0441 | 0.0380 | 0.0363 |
| | Hosseini *et al.* (2011) | = 0 | 0.0577 | 0.0490 | 0.0442 | 0.0381 | 0.0364 |
| | Matsunaga (2008) | ≠ 0 | 0.0577 | 0.0491 | 0.0442 | 0.0381 | 0.0364 |
| | Sheikholeslami and Saidi (2013) | ≠ 0 | 0.0577 | 0.0491 | 0.0442 | 0.0381 | 0.0364 |
| | Belabed *et al.* (2014) | ≠ 0 | 0.0578 | 0.0494 | 0.0449 | 0.0389 | 0.0368 |
| | Akavci and Tanrikulu (2015) | = 0 | 0.0577 | 0.0490 | 0.0442 | 0.0380 | 0.0363 |
| | Present | = 0 | 0.0577 | 0.0490 | 0.0442 | 0.0381 | 0.0364 |
| | Akavci and Tanrikulu (2015) | ≠ 0 | 0.0578 | 0.0494 | 0.0449 | 0.0389 | 0.0368 |
| | Present | ≠ 0 | 0.0578 | 0.0494 | 0.0449 | 0.0389 | 0.0368 |
| 20 | Benachour *et al.* (2011) | = 0 | 0.0148 | 0.0125 | 0.0113 | 0.0098 | 0.0094 |
| | Hosseini *et al.* (2011) | = 0 | 0.0148 | 0.0125 | 0.0113 | 0.0098 | 0.0094 |
| | Sheikholeslami and Saidi (2013) | ≠ 0 | 0.0148 | 0.0125 | 0.0113 | 0.0098 | 0.0094 |
| | Belabed *et al.* (2014) | ≠ 0 | 0.0148 | 0.0126 | 0.0115 | 0.0100 | 0.0095 |
| | Akavci and Tanrikulu (2015) | = 0 | 0.0148 | 0.0125 | 0.0113 | 0.0098 | 0.0094 |
| | Present | = 0 | 0.0148 | 0.0125 | 0.0113 | 0.0098 | 0.0094 |
| | Akavci and Tanrikulu (2015) | ≠ 0 | 0.0148 | 0.0126 | 0.0115 | 0.0100 | 0.0095 |
| | Present | ≠ 0 | 0.0148 | 0.0126 | 0.0115 | 0.0100 | 0.0095 |

Table 10 Comparison of the first three non-dimensional natural frequencies $\bar{\omega} = \omega a^2/h \sqrt{\rho_C / E_C}$ for Al/$Al_2O_3$ square plate ($a/h$=10)

| Mode ($m$, $n$) | Theory | $\varepsilon_z$ | $K$ | | | | |
|---|---|---|---|---|---|---|---|
| | | | 0 | 0.5 | 1 | 4 | 10 |
| (1, 1) | Benachour *et al.* (2011) | = 0 | 5.7690 | 4.9000 | 4.4160 | 3.8040 | 3.6350 |
| | Matsunaga (2008) | ≠ 0 | 5.7777 | 4.9170 | 4.4270 | 3.8110 | 3.6420 |
| | Belabed *et al.* (2014) | ≠ 0 | 5.7800 | 4.9400 | 4.4900 | 3.8900 | 3.6800 |
| | Akavci and Tanrikulu (2015) | = 0 | 5.7695 | 4.9015 | 4.4193 | 3.8064 | 3.6365 |
| | Present | = 0 | 5.7695 | 4.9016 | 4.4195 | 3.8070 | 3.6368 |
| | Akavci and Tanrikulu (2015) | ≠ 0 | 5.7807 | 4.9410 | 4.4907 | 3.8934 | 3.6827 |
| | Present | ≠ 0 | 5.7794 | 4.9401 | 4.4900 | 3.8931 | 3.6826 |
| (1, 2) | Benachour *et al.* (2011) | = 0 | 13.7600 | 11.7310 | 10.5760 | 9.0120 | 8.5570 |
| | Matsunaga (2008) | ≠ 0 | 13.8100 | 11.8000 | 10.6300 | 9.0450 | 8.5880 |
| | Belabed *et al.* (2014) | ≠ 0 | 13.8000 | 11.8400 | 10.7700 | 9.2300 | 8.6800 |
| | Akavci and Tanrikulu (2015) | = 0 | 13.7650 | 11.7390 | 10.5900 | 9.0224 | 8.5613 |
| | Present | = 0 | 13.7653 | 11.7407 | 10.5934 | 9.0274 | 8.5637 |
| | Akavci and Tanrikulu (2015) | ≠ 0 | 13.8170 | 11.8510 | 10.7730 | 9.2314 | 8.6768 |
| | Present | ≠ 0 | 13.8132 | 11.8496 | 10.7728 | 9.2337 | 8.6778 |
| (2, 2) | Benachour *et al.* (2011) | = 0 | 21.1250 | 18.0550 | 16.2820 | 13.7560 | 12.9950 |
| | Matsunaga (2008) | ≠ 0 | 21.2100 | 18.1900 | 16.4000 | 13.8300 | 13.0600 |
| | Belabed *et al.* (2014) | ≠ 0 | 21.2100 | 18.2500 | 16.5900 | 14.0900 | 13.1800 |
| | Akavci and Tanrikulu (2015) | = 0 | 21.1270 | 18.0730 | 16.3130 | 13.7770 | 13.0020 |
| | Present | = 0 | 21.1262 | 18.0784 | 16.3235 | 13.7922 | 13.0096 |
| | Akavci and Tanrikulu (2015) | ≠ 0 | 21.2370 | 18.2680 | 16.6090 | 14.0990 | 13.1860 |
| | Present | ≠ 0 | 21.2306 | 18.2676 | 16.6128 | 14.1090 | 13.1898 |

The next two examples are established for Al/$Al_2O_3$ thick FG square plates. In Table 9, non-dimensional fundamental frequencies of a square plate are calculated for various values of the material index and different $a/h$ ratios and compared with FSDT of Zhu and Liew (2011), 2D shear deformation theory of Benachour *et al.* (2011) and quasi-3D shear deformation theories of Hosseini *et al.* (2011), Matsunaga (2008), Sheikholeslami and Saidi (2013), Belabed *et al.* (2014) and and Akavci and Tanrikulu (2015). Again, it can be seen that the computed results correlate exceptionally well with the other quasi-3D results, even for very thick plates. The table demonstrates that, fundamental frequencies increase with the increase in the thickness of plate and diminish with the increase of material index. In Table 10, to check the higher order modes for FG plates, the first three frequencies of the Al/$Al_2O_3$ FG square plates are calculated and compared with the 2D HSDT of Benachour *et al.* (2011) and quasi-3D HSDTs of Matsunaga (2008), Belabed *et al.* (2014) and Akavci and Tanrikulu (2015). As it is observed from the table, the proposed theories are in good agreement with those reported by the other quasi-3D models of Matsunaga (2008), Belabed *et al.* (2014) and Akavci and Tanrikulu (2015), particularly at the higher modes of vibration. It is observed from the tables that when the influences of normal deformations are neglected, the natural frequencies of FG plates are found lower.

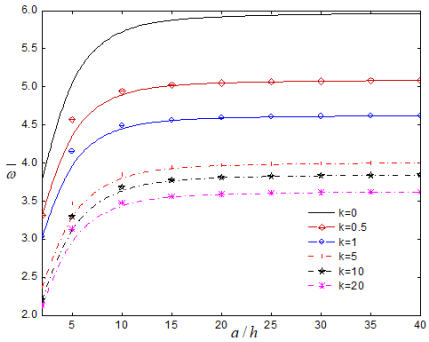


Fig. 4 Effect of the side-to-thickness ratio $a/h$ and power-law index $k$ on the non-dimensional fundamental frequency $\bar{\omega}$ of FG square plates

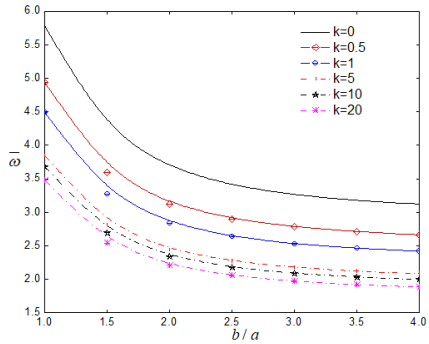


Fig. 5 Effect of the aspect ratio $b/a$ and power-law index $k$ on the non-dimensional fundamental frequency $\bar{\omega}$ of FG plates ($a/h$=10).

Fig. 4 presents the variation of the non-dimensional frequency versus the thickness ratio $a/h$ for different power-law index $k$. It can be seen that the non-dimensional frequency decreases with increasing the material index $k$.

Fig. 5 shows the variation of the non-dimensional frequency versus the aspect ratio $b/a$ for different material index $k$. It can be observed that the increase of $b/a$ leads to a reduction of the non-dimensional frequency.

## 5. Conclusions

This paper presents both bending and free vibration investigations for FG plates using a novel non-polynomial quasi-3D HSDTs. The kinematic is developed by considering further simplifying assumptions to the existing HSDTs, with the use of an undetermined integral term leading to only five unknowns. The equations of motion have been determined by the Hamilton principle. Double Fourier series have been employed to solve the partial differential equations. The accuracy of proposed theory has been demonstrated via the results computed by present model compared with the results of the other theories.

The results determined by the proposed method can be summarized as follows:

• Through all the comparative investigations, it can be seen that the proposed theory proves good agreement with that of the results of other 2D and quasi-3D HSDTs.

• The results demonstrate that the 2D and quasi-3D HSDTs have almost identical results for thin plates. For the thick and moderately thick plates, however, it has been observed from the comparison investigations that the quasi-3D theories which account for the stretching effects, can predict the bending and dynamic behavior more accurately compared to other HDSTs. So, it is relevant to conclude that the influence of thickness stretching on static and dynamic behavior of FG plates are just as considerable as the influence of transverse shear strains and must be taken into account.

• The proposed quasi-3D HSDT contains five unknowns, but gives results comparable with those predicted by existing quasi-3D theories having more number of unknowns (e.g., quasi-3D theories of Neves *et al.* (2012ab) with nine unknowns and Akavci and Tanrikulu (2015) with six unknowns).

• Although the transverse stress components can be computed from the constitutive equations, these stresses may not satisfy the stress boundary conditions on the upper and lower surfaces of the plate. So, the transverse stress components may be determined by employing equilibrium equations of 3D elasticity theory as satisfying the stress boundary conditions.

• The fundamental frequencies of plate decrease with the increase of material index. Although increasing value of material index causes to reduce in the natural frequency, the influence of the value of material index more than 5 is negligible.

• The small difference between the proposed 2D and quasi-3D HSDT results is due to the ignoring the thickness stretching influence. If the influences of normal deformations ignored, the fundamental frequencies of FG plates are found lower.

• The thickness stretching influence is more pronounced for thick plates and it needs to be taken in consideration in the modeling.

## References

Abdelhak, Z., Hadji, L., Hassaine Daouadji, T. and Adda Bedia, E.A. (2016), "Thermal buckling response of functionally graded sandwich plates with clamped boundary conditions", *Smart Struct. Syst.*, **18**(2), 267-291.

Ahmed, A. (2014), "Post buckling analysis of sandwich beams with functionally graded faces using a consistent higher order theory", *J. Civ. Struct. Environ.*, **4**(2), 59-64.

Ahouel, M., Houari, M.S.A., Adda Bedia, E.A. and Tounsi, A. (2016) "Size-dependent mechanical behavior of functionally graded trigonometric shear deformable nanobeams including neutral surface position concept", *Steel Compos. Struct.*, **20**(5), 963-981.

Ait Amar Meziane, M., Abdelaziz, H.H. and Tounsi, A. (2014), "An efficient and simple refined theory for buckling and free vibration of exponentially graded sandwich plates under various boundary conditions", *J. Sandw. Struct. Mater.*, **16**(3), 293-318.

Ait Atmane, H., Tounsi, A. and Bernard, F. (2017), "Effect of thickness stretching and porosity on mechanical response of a functionally graded beams resting on elastic foundations", *J. Mech. Mater. Des.*, **13**(1), 71-84.

Ait Atmane, H., Tounsi, A., Bernard, F. and Mahmoud, S.R. (2015), "A computational shear displacement model for vibrational analysis of functionally graded beams with

porosities", *Steel Compos. Struct.*, **19**(2), 369-384.
Ait Yahia, S., Ait Atmane, H., Houari, M.S.A. and Tounsi, A. (2015), "Wave propagation in functionally graded plates with porosities using various higher-order shear deformation plate theories", *Struct. Eng. Mech.*, **53**(6), 1143-1165.
Akavci, S.S. and Tanrikulu, A.H. (2015), "Static and free vibration analysis of functionally graded plates based on a new quasi-3D and 2D shear deformation theories", *Compos. Part B Eng.*, **83**, 203- 215.
Aldousari, S.M. (2017), "Bending analysis of different material distributions of functionally graded beam", *Appl. Phys. A Mater. Sci. Proc.*, **123**(4), 296.
Alijani, F. and Amabili, M. (2014), "Effect of thickness deformation on large-amplitude vibrations of functionally graded rectangular plates", *Compos. Struct.*, **113**, 89-107.
Arani, A.J. and Kolahchi, R. (2016), "Buckling analysis of embedded concrete columns armed with carbon nanotubes", *Comput. Concrete*, **17**(5), 567-578.
Attia, A., Tounsi, A., Adda Bedia, E.A. and Mahmoud, S.R. (2015), "Free vibration analysis of functionally graded plates with temperature-dependent properties using various four variable refined plate theories", *Steel Compos. Struct.*, **18**(1), 187-212.
Bao, G. and Wang, L. (1995), "Multiple cracking in functionally graded ceramic/metal coatings", *J. Solid. Struct.*, **32**(19), 2853-2871 .
Barati, M.R. and Shahverdi, H. (2016), "A four-variable plate theory for thermal vibration of embedded FG nanoplates under non-uniform temperature distributions with different boundary conditions", *Struct. Eng. Mech.*, **60**(4), 707-727.
Barka, M., Benrahou, K.H., Bakora, A. and Tounsi, A. (2016), "Thermal post-buckling behavior of imperfect temperature-dependent sandwich FGM plates resting on Pasternak elastic foundation", *Steel Compos. Struct.*, **22**(1), 91-112.
Baseri, V., Jafari, G.R.S. and Kolahchi, R. (2016), "Analytical solution for buckling of embedded laminated plates based on higher order shear deformation plate theory", *Steel Compos. Struct.*, **21**(4), 883-919.
Belabed, Z., Houari, M.S.A., Tounsi, A., Mahmoud, S.R. and Anwar Bég, O. (2014), "An efficient and simple higher order shear and normal deformation theory for functionally graded material (FGM) plates", *Compos. Part B Eng.*, **60**, 274-283.
Beldjelili, Y., Tounsi, A. and Mahmoud, S.R. (2016), "Hygro-thermo-mechanical bending of S-FGM plates resting on variable elastic foundations using a four-variable trigonometric plate theory", *Smart Struct. Syst.*, **18**(4), 755-786.
Belkorissat, I., Houari, M.S.A., Tounsi, A., Adda Bedia, E.A. and Mahmoud, S.R. (2015), "On vibration properties of functionally graded nano-plate using a new nonlocal refined four variable model", *Steel Compos. Struct.*, **18**(4), 1063-1081.
Bellifa, H., Benrahou, K.H., Bousahla, A.A., Tounsi, A. and Mahmoud, S.R. (2017), "A nonlocal zeroth-order shear deformation theory for nonlinear postbuckling of nanobeams", *Struct. Eng. Mech.*, **62**(6), 695-702.
Bellifa, H., Benrahou, K.H., Hadji, L., Houari, M.S.A. and Tounsi, A. (2016), "Bending and free vibration analysis of functionally graded plates using a simple shear deformation theory and the concept the neutral surface position", *J. Braz. Soc. Mech. Sci. Eng.*, **38**(1), 265-275.
Benachour, A., Daouadji Tahar, H., Ait Atmane, H., Tounsi, A. and Meftah, S.A. (2011), "A four variable refined plate theory for free vibrations of functionally graded plates with arbitrary gradient", *Compos. Part B Eng.*, **42**(6), 1386-1394.
Benahmed, A., Houari, M.S.A., Benyoucef, S., Belakhdar, K. and Tounsi, A. (2017), "A novel quasi-3D hyperbolic shear deformation theory for functionally graded thick rectangular plates on elastic foundation", *Geomech. Eng.*, **12**(1), 9-34.
Benbakhti, A., Bachir Bouiadjra, M., Retiel, N. and Tounsi, A. (2016), "A new five unknown quasi-3D type HSDT for thermomechanical bending analysis of FGM sandwich plates", *Steel Compos. Struct.*, **22**(5), 975-999.
Benchohra, M., Driz, H., Bakora, A., Tounsi, A., Adda Bedia, E.A. and Mahmoud, S.R. (2017), "A new quasi-3D sinusoidal shear deformation theory for functionally graded plates", *Struct. Eng. Mech.*, **65**(1), 19-31.
Benferhat, R., Hassaine Daouadji, T., Hadji, L. and Said Mansour, M. (2016), "Static analysis of the FGM plate with porosities", *Steel Compos. Struct.*, **21**(1), 123-136.
Bennoun, M., Houari, M.S.A. and Tounsi, A. (2016), "A novel five variable refined plate theory for vibration analysis of functionally graded sandwich plates", *Mech. Adv. Mater. Struct.*, **23**(4), 423-431.
Benveniste, Y. (1987), "A new approach to the application of Mori-Tanaka's theory in composite materials", *Mech. Mater.*, **6**(2), 147-157.
Bessaim, A., Houari, M.S.A., Tounsi, A., Mahmoud, S.R. and Adda Bedia, E.A. (2013), "A new higher order shear and normal deformation theory for the static and free vibration analysis of sandwich plates with functionally graded isotropic face sheets", *J. Sandw. Struct. Mater.*, **15**(6), 671-703.
Besseghier, A., Houari, M.S.A., Tounsi, A. and Mahmoud, S.R. (2017), "Free vibration analysis of embedded nanosize FG plates using a new nonlocal trigonometric shear deformation theory", *Smart Struct. Syst.*, **19**(6), 601-614.
Bilouei, B.S., Kolahchi, R. and Bidgoli, M.R. (2016), "Buckling of concrete columns retrofitted with Nano-Fiber Reinforced Polymer (NFRP)", *Comput. Concrete*, **18**(5), 1053-1063.
Bouafia, K., Kaci, A., Houari, M.S.A., Benzair, A. and Tounsi, A. (2017), "A nonlocal quasi-3D theory for bending and free flexural vibration behaviors of functionally graded nanobeams", *Smart Struct. Syst.*, **19**(2), 115-126.
Bouderba, B., Houari, M.S.A. and Tounsi, A. (2013), "Thermomechanical bending response of FGM thick plates resting on Winkler-Pasternak elastic foundations", *Steel Compos. Struct.*, **14**(1), 85-104.
Bouderba, B., Houari, M.S.A. and Tounsi, A. and Mahmoud, S.R. (2016), "Thermal stability of functionally graded sandwich plates using a simple shear deformation theory", *Struct. Eng. Mech.*, **58**(3), 397-422.
Boukhari, A., Ait Atmane, H., Tounsi, A., Adda Bedia, E.A. and Mahmoud, S.R. (2016), "An efficient shear deformation theory for wave propagation of functionally graded material plates", *Struct. Eng. Mech.*, **57**(5), 837-859.
Bounouara, F., Benrahou, K.H., Belkorissat, I. and Tounsi, A. (2016), "A nonlocal zeroth-order shear deformation theory for free vibration of functionally graded nanoscale plates resting on elastic foundation", *Steel Compos. Struct.*, **20**(2), 227-249.
Bourada, F., Amara, K. and Tounsi, A. (2016), "Buckling analysis of isotropic and orthotropic plates using a novel four variable refined plate theory", *Steel Compos. Struct.*, **21**(6), 1287-1306.
Bourada, M., Kaci, A., Houari, M.S.A. and Tounsi, A. (2015), "A new simple shear and normal deformations theory for functionally graded beams", *Steel Compos. Struct.*, **18**(2), 409-423.
Bousahla, A.A., Benyoucef, S., Tounsi, A. and Mahmoud, S.R. (2016), "On thermal stability of plates with functionally graded coefficient of thermal expansion", *Struct. Eng. Mech.*, **60**(2), 313-335.
Bousahla, A.A., Houari, M.S.A., Tounsi, A. and Adda Bedia, E.A. (2014), "A novel higher order shear and normal deformation theory based on neutral surface position for bending analysis of advanced composite plates", *J. Comput. Meth.*, **11**(6), 1350082.
Carrera, E., Brischetto, S., Cinefra, M. and Soave, M. (2011), "Effects of thickness stretching in functionally graded plates

and shells", *Compos. Part B Eng.*, **42**(2), 123-133.
Chikh, A., Bakora, A., Heireche, H., Houari, M.S.A., Tounsi, A. and Adda Bedia, E.A. (2016), "Thermo-mechanical postbuckling of symmetric S-FGM plates resting on Pasternak elastic foundations using hyperbolic shear deformation theory", *Struct. Eng. Mech.*, **57**(4), 617-639.
Chikh, A., Tounsi, A., Hebali, H. and Mahmoud, S.R. (2017), "Thermal buckling analysis of cross-ply laminated plates using a simplified HSDT", *Smart Struct. Syst.*, **19**(3), 289-297.
Delale, F. and Erdogan, F. (1983), "The crack problem for a nonhomogeneous plane", *J. Appl. Mech.*, **50**(3), 609-614.
Draiche, K., Tounsi, A. and Mahmoud, S.R. (2016), "A refined theory with stretching effect for the flexure analysis of laminated composite plates", *Geomech. Eng.*, **11**(5), 671-690.
El-Haina, F., Bakora, A., Bousahla, A.A., Tounsi, A. and Mahmoud, S.R. (2017), "A simple analytical approach for thermal buckling of thick functionally graded sandwich plates", *Struct. Eng. Mech.*, **63**(5), 585-595.
El-Hassar, S.M., Benyoucef, S., Heireche, H. and Tounsi, A. (2016), "Thermal stability analysis of solar functionally graded plates on elastic foundation using an efficient hyperbolic shear deformation theory", *Geomech. Eng.*, **10**(3), 357-386.
Fahsi, A., Tounsi, A., Hebali, H.,Chikh, A., AddaBedia, E.A. and Mahmoud, S.R. (2017), "A four variable refined *n*th-order shear deformation theory for mechanical and thermal buckling analysis of functionally graded plates", *Geomech. Eng.*, **13**(3), 385-410.
Fekrar, A., Houari, M.S.A., Tounsi, A. and Mahmoud, S.R. (2014), "A new five-unknown refined theory based on neutral surface position for bending analysis of exponential graded plates", *Meccanica*, **49**(4), 795-810.
Ghorbanpour Arani, A., Kolahchi, R. and Esmailpour, M. (2016a), "Nonlinear vibration analysis of piezoelectric plates reinforced with carbon nanotubes using DQM", *Smart Struct. Syst.*, **18**(4), 787-800.
Ghorbanpour Arani, A., Cheraghbak, A. and Kolahchi, R. (2016b), "Dynamic buckling of FGM viscoelastic nano-plates resting on orthotropic elastic medium based on sinusoidal shear deformation theory", *Struct. Eng. Mech.*, **60**(3), 489-505.
Gunes, R., Aydin, M., Apalak, M.K. and Reddy, J.N. (2014), "Experimental and numerical investigations of low velocity impact on functionally graded circular plates", *Compos. Part B Eng.*, **59**, 21-32.
Hadji, L., Hassaine Daouadji, T. and Adda Bedia, E. (2015), "A refined exponential shear deformation theory for free vibration of FGM beam with porosities", *Geomech. Eng.*, **9**(3), 361 - 372.
Hadji, L., Hassaine Daouadji, T., Ait Amar Meziane, M., Tlidji, Y. and Adda Bedia, E.A. (2016), "Analysis of functionally graded beam using a new first-order shear deformation theory", *Struct. Eng. Mech.*, **57**(2), 315-325.
Hamidi, A., Houari, M.S.A., Mahmoud, S.R. and Tounsi, A. (2015), "A sinusoidal plate theory with 5-unknowns and stretching effect for thermomechanical bending of functionally graded sandwich plates", *Steel Compos. Struct.*, **18**(1), 235-253.
Hebali, H., Bakora, A., Tounsi, A. and Kaci, A. (2016), "A novel four variable refined plate theory for bending, buckling, and vibration of functionally graded plates", *Steel Compos. Struct.*, **22**(3), 473-495.
Hebali, H., Tounsi, A., Houari, M.S.A., Bessaim, A. and Adda Bedia, E.A. (2014), "A new quasi-3D hyperbolic shear deformation theory for the static and free vibration analysis of functionally graded plates", *J. Eng. Mech.*, **140**(2), 374- 383.
Hosseini-Hashemi, S.H., Fadaee, M. and Atashipour, S.R. (2011), "Study on the free vibration of thick functionally graded rectangular plates according to a new exact closed form procedure", *Compos. Struct.*, **93**(2), 722-735.
Houari, M.S.A., Tounsi, A., Bessaim, A. and Mahmoud, S.R. (2016), "A new simple three-unknown sinusoidal shear deformation theory for functionally graded plates", *Steel Compos. Struct.*, **22**(2), 257-276.
Jha, D.K., Kant, T. and Singh, R.K. (2013), "Free vibration response of functionally graded thick plates with shear and normal deformations effects", *Compos. Struct.*, **96**, 799-823.
Kar, V.R. and Panda, S.K. (2015a), "Free vibration responses of temperature dependent functionally graded curved panels under thermal environment", *Lat. Am. J. Solid. Struct.*, **12**(11), 2006-2024.
Kar, V.R. and Panda, S.K. (2015b), "Large deformation bending analysis of functionally graded spherical shell using FEM", *Struct. Eng. Mech.*, **53**(4), 661-679.
Kar, V.R., Mahapatra, T.R. and Panda, S.K. (2015), "Nonlinear flexural analysis of laminated composite flat panel under hygro-thermo-mechanical loading", *Steel Compos. Struct.*, **19**(4), 1011-1033.
Kashtalyan, M. (2004), "Three-dimensional solution for bending of functionally graded rectangular plates", *Eur. J. Mech. A Solid.*, **23**(5), 853-864.
Khetir, H., Bachir Bouiadjra, M., Houari, M.S.A., Tounsi, A. and Mahmoud, S.R. (2017), "A new nonlocal trigonometric shear deformation theory for thermal buckling analysis of embedded nanosize FG plates", *Struct. Eng. Mech.*, **64**(4), 391-402.
Klouche, F., Darcherif, L., Sekkal, M., Tounsi, A. and Mahmoud, S.R. (2017), "An original single variable shear deformation theory for buckling analysis of thick isotropic plates", *Struct. Eng. Mech.*, **63**(4), 439-446.
Kolahchi, R. and Moniri Bidgoli, A.M. (2016), "Size-dependent sinusoidal beam model for dynamic instability of single-walled carbon nanotubes", *Appl. Math. Mech.*, **37**(2), 265-274.
Kolahchi, R., Hosseini, H. and Esmailpour, M. (2016a), "Differential cubature and quadrature-Bolotin methods for dynamic stability of embedded piezoelectric nanoplates based on visco-nonlocal-piezoelasticity theories", *Compos. Struct.*, **157**, 174-186.
Kolahchi, R., Safari, M. and Esmailpour, M. (2016b), "Dynamic stability analysis of temperature-dependent functionally graded CNT-reinforced visco-plates resting on orthotropic elastomeric medium", *Compos. Struct.*, **150**, 255-265.
Kolahchi, R., Zarei, M.S., Hajmohammad, M.H. and Oskouei, A.N. (2017), "Visco-nonlocal-refined Zigzag theories for dynamic buckling of laminated nanoplates using differential cubature-Bolotin methods", *Thin-Wall. Struct.*, **113**, 162-169.
Laoufi, I., Ameur, M., Zidi, M., Adda Bedia, E.A. and Bousahla, A.A. (2016), "Mechanical and hygrothermal behaviour of functionally graded plates using a hyperbolic shear deformation theory", *Steel Compos. Struct.*, **20**(4), 889-911.
Larbi Chaht, F., Kaci, A., Houari, M.S.A., Tounsi, A., Anwar Bég, O. and Mahmoud, S.R. (2015), "Bending and buckling analyses of functionally graded material (FGM) size-dependent nanoscale beams including the thickness stretching effect", *Steel Compos. Struct.*, **18**(2), 425-442.
Madani, H., Hosseini, H. and Shokravi, M. (2016), "Differential cubature method for vibration analysis of embedded FG-CNT-reinforced piezoelectric cylindrical shells subjected to uniform and non-uniform temperature distributions", *Steel Compos. Struct.*, **22**(4), 889-913.
Mahi, A., Adda Bedia, E.A. and Tounsi, A. (2015), "A new hyperbolic shear deformation theory for bending and free vibration analysis of isotropic, functionally graded, sandwich and laminated composite plates", *Appl. Math. Modell.*, **39**(9), 2489-2508.
Mantari, J.L. and Soares, C.G. (2013), "A novel higher-order shear deformation theory with stretching effect for functionally graded plates", *Compos. Part B Eng.*, **45**(1), 268-281.
Matsunaga, H. (2008), "Free vibration and stability of functionally

graded plates according to a 2-D higher-order deformation theory", *Compos. Struct.*, **82**(4), 499-512.
Matsunaga, H. (2009), "Stress analysis of functionally graded plates subjected to thermal and mechanical loadings", *Compos. Struct.*, **87**(4), 344-357.
Meksi, R, Benyoucef, S., Mahmoudi, A., Tounsi, A., Adda Bedia, E.A. and Mahmoud, SR. (2017), "An analytical solution for bending, buckling and vibration responses of FGM sandwich plates", *J. Sandw. Struct. Mater.*, 1099636217698443.
Menasria, A., Bouhadra, A., Tounsi, A., Bousahla, A.A. and Mahmoud, S.R. (2017), "A new and simple HSDT for thermal stability analysis of FG sandwich plates", *Steel Compos. Struct.*, **25**(2), 157-175.
Meradjah, M., Kaci, A., Houari, M.S.A., Tounsi, A., Mahmoud, S.R. (2015), "A new higher order shear and normal deformation theory for functionally graded beams", *Steel Compos. Struct.*, **18**(3), 793-809.
Mori, T. and Tanaka, K. (1973), "Average stress in matrix and average elastic energy of materials with misfitting inclusions", *Acta Metall.*, **21**(5), 571-574.
Mouaici, F., Benyoucef, S., Ait Atmane, H. and Tounsi, A. (2016), "Effect of porosity on vibrational characteristics of non-homogeneous plates using hyperbolic shear deformation theory", *Wind Struct.*, **22**(4), 429-454.
Mouffoki, A., Adda Bedia, E.A., Houari, M.S.A., Tounsi, A. and Mahmoud, S.R. (2017), "Vibration analysis of nonlocal advanced nanobeams in hygro-thermal environment using a new two-unknown trigonometric shear deformation beam theory", *Smart Struct. Syst.*, **20**(3), 369-383.
Neves, A.M.A., Ferreira, A.J.M., Carrera, E., Cinefra, M., Roque, C.M.C., Jorge, R.M.N. and Soares, C.M.M. (2012b), "A quasi-3D hyperbolic shear deformation theory for the static and free vibration analysis of functionally graded plates", *Compos. Struct.*, **94**(5), 1814-1825.
Neves, A.M.A., Ferreira, A.J.M., Carrera, E., Roque, C.M.C., Cinefra, M., Jorge, R.M.N. and Soares, C.M.M. (2012a), "A quasi-3D sinusoidal shear deformation theory for the static and free vibration analysis of functionally graded plates", *Compos. Part B Eng.*, **43**(2), 711-725.
Orakdöğen, E., Küçükarslan, S., Sofiyev, A. and Omurtag, M.H. (2010), "Finite element analysis of functionally graded plates for coupling effect of extension and bending", *Meccanica*, **45**(1), 63-72.
Rahmani, O., Refaeinejad, V. and Hosseini, S.A.H. (2017), "Assessment of various nonlocal higher order theories for the bending and buckling behavior of functionally graded nanobeams", *Steel Compos. Struct.*, **23**(3), 339-350.
Sheikholeslami, S.A. and Saidi, A.R. (2013), "Vibration analysis of functionally graded rectangular plates resting on elastic foundation using higher-order shear and normal deformable plate theory", *Compos. Struct.*, **106**, 350-361.
Sofiyev, A.H. and Kuruoglu, N. (2015), "On a problem of the vibration of functionally graded conical shells with mixed boundary conditions", *Compos. Part B Eng.*, **70**, 122-130.
Srinivas, S., Rao, C.J. and Rao, A.K. (1970), "An exact analysis for vibration of simply supported homogeneous and laminated thick rectangular plates", *J. Sound Vib.*, **12**(2), 187-199.
Swaminathan, K. and Naveenkumar, D.T. (2014), "Higher order refined computational models for the stability analysis of FGM plates: Analytical solutions", *Eur. J. Mech. A Solid.*, **47**, 349-361.
Taibi, F.Z., Benyoucef, S., Tounsi, A., Bachir Bouiadjra, R., Adda Bedia, E.A. and Mahmoud, S.R. (2015), "A simple shear deformation theory for thermo-mechanical behaviour of functionally graded sandwich plates on elastic foundations", *J. Sandw. Struct. Mater.*, **17**(2), 99-129.
Tamijani, A.Y. and Kapania, R.K. (2012), "Vibration analysis of curvilinearly-stiffened functionally graded plate using element free Galerkin method", *Mech. Adv. Mater. Struct.*, **19**(1-3), 100-108.
Tounsi, A., Houari, M.S.A., Benyoucef, S. and Adda Bedia, E.A. (2013), "A refined trigonometric shear deformation theory for thermoelastic bending of functionally graded sandwich plates", *Aerosp. Sci. Technol.*, **24**(1), 209-220.
Vaghefi, R., Baradaran, G.H. and Koohkan, H. (2010), "Three-dimensional static analysis of thick functionally graded plates by using meshless local Petrov-Galerkin (MLPG) method", *Eng. Anal. Bound. Elem.*, **34**(6), 564-573.
Zafarmand, H. and Kadkhodayan, M. (2015), "Three dimensional elasticity solution for static and dynamic analysis of multi-directional functionally graded thick sector plates with general boundary conditions", *Compos. Part B Eng.*, **69**, 592-602.
Zamanian, M., Kolahchi, R. and Bidgoli, M.R. (2017), "Agglomeration effects on the buckling behaviour of embedded concrete columns reinforced with SiO2 nano-particles", *Wind Struct.*, **24**(1), 43-57.
Zemri, A., Houari, M.S.A., Bousahla, A.A. and Tounsi, A. (2015), "A mechanical response of functionally graded nanoscale beam: An assessment of a refined nonlocal shear deformation theory beam theory", *Struct. Eng. Mech.*, **54**(4), 693-710.
Zenkour, A.M. (2007), "Benchmark trigonometric and 3-D elasticity solutions for an exponentially graded thick rectangular plate", *Arch. Appl. Mech.*, **77**(4), 197-214.
Zhang, H., Jiang, J.K. and Zhang, Z.C. (2014), "Three-dimensional elasticity solutions for bending of generally supported thick functionally graded plates", *Appl. Math. Mech.*, **35**(11), 1467-1478.
Zhao, X., Lee, Y.Y. and Liew, K.M. (2009), "Free vibration analysis of functionally graded plates using the element-free kp-Ritz method", *J. Sound Vib.*, **319**(3-5), 918-939.
Zhu, P. and Liew, K.M. (2011), "Free vibration analysis of moderately thick functionally graded plates by local Kriging meshless method", *Compos. Struct.*, **93**(11), 2925-2944.
Zidi, M., Houari, M.S.A., Tounsi, A., Bessaim, A. and Mahmoud, S.R. (2017), "A novel simple two-unknown hyperbolic shear deformation theory for functionally graded beams", *Struct. Eng. Mech.*, **64**(2), 145-153.
Zidi, M., Tounsi, A., Houari M.S.A., Adda Bedia, E.A. and Anwar Bég, O. (2014), "Bending analysis of FGM plates under hygro-thermo-mechanical loading using a four variable refined plate theory", *Aerosp. Sci. Technol.*, **34**, 24-34.

*CC*